Cell Reports

VIROLOGICAL AND IMMUNOLOGICAL FEATURES OF SARS-CoV-2 INFECTED CHILDREN DEVELOPING SPECIFIC AND NEUTRALIZING ANTIBODIES

--Manuscript Draft--

Manuscript Number:	CELL-REPORTS-D-20-04757
Full Title:	VIROLOGICAL AND IMMUNOLOGICAL FEATURES OF SARS-CoV-2 INFECTED CHILDREN DEVELOPING SPECIFIC AND NEUTRALIZING ANTIBODIES
Article Type:	Research Article
Keywords:	SARS-CoV-2; pediatric COVID-19; anti-SARS-CoV-2 antibodies; Ab-mediated neutralization activity; antigen-specific CD4 T cells; antigen-specific B-cells.
Corresponding Author:	Paolo Palma, MD, PhD Ospedale Pediatrico Bambino Gesù Rome, Italy ITALY
First Author:	Nicola Cotugno
Order of Authors:	Nicola Cotugno
	Alessandra Ruggiero, PhD
	Francesco Bonfante
	Maria Raffella Pertrara
	Sonia Zicari
	Giuseppe Rubens Pascucci
	Paola Zangari
	Maria Antonietta De Ioris
	Veronica Santilli
	Emma Manno
	Donato Amodio
	Alessio Bortolami
	Matteo Pagliari
	Carlo Concato
	Giulia Linardos
	Andrea Campana
	Daniele Donà
	Carlo Giaquinto
	Petter Brodin
	Paolo Rossi
	Anita De Rossi
	Paolo Palma
Abstract:	As the global COVID-19 pandemic progresses and with the school reopening, it is paramount to gain knowledge on adaptive immunity to SARS-CoV-2 in children in order to define possible immunization strategies and reconsider pandemic control measures. We analyzed anti-SARS-CoV-2 antibodies (Ab) and their neutralizing activity (PRNT) in 42 COVID-19-infected children 7 days after symptoms onset. Individuals with specific humoral responses presented faster virus clearance, and lower viral load associated to a reduced in vitro infectivity. We demonstrated that the frequencies of SARS-CoV-2 specific CD4-CD40L+ T-cells and Spike specific B-cells

	were associated with the anti-SARS-CoV-2 Ab and the magnitude of neutralizing activity. The plasma proteome confirmed the association between cellular and humoral SARS-CoV-2 immunity, with PRNT+ patients showing higher viral signal transduction molecules (SLAMF1, CD244, CLEC4G). This work shed lights on cellular and humoral anti-SARS-CoV-2 responses in children which may drive future vaccination trials endpoints and quarantine measures policies.
Suggested Reviewers:	Alba Grifoni agrifoni@lji.org Experience in SARS-CoV-2 specific CD4 T cells
	Pratip K Chattopadhyay Pratip.Chattopadhyay@nyulangone.org Setting up of the CD40L to detect antigen specific CD4 T-cells
	Alberto Mantovani alnerto.mantovani@hunimed.eu Expert immunologists
	Stoyan Dimitrov stoyan.dimitrov@uni-tuebingen.de Extensive experience in Ag-specific immunity
	Luigi Daniele Notarangelo luigi.notarangelo2@nih.gov Experience in molecular and cellular mechanisms underlying immune dysregulation
Opposed Reviewers:	

Bambino Gesù
OSPEDALE PEDIATRICO

Università
degli Studi di Roma Tor Vergata

September 14th, 2020

Dear Editor,

We are submitting a manuscript entitled *"VIROLOGICAL AND IMMUNOLOGICAL FEATURES OF SARS-Cov-2 INFECTED CHILDREN DEVELOPING NEUTRALIZING ANTIBODIES*" for consideration for publication as research article in Cell Reports.

In collaboration with Petter Brodin group, we recently described in Cell journal the immunological features of multi inflammatory syndrome (MIS-C) affecting a minor subgroup of children infected by SARS-CoV-2 (Consilio CR, Cell, 2020). Nonetheless the majority of children affected by SARS-CoV-2 do not resemble MIS-C, presenting a milder course of disease.

As the global COVID-19 pandemic progresses and with the forthcoming school reopening, children could represent a major source of infection. It is thus paramount to gain knowledge on adaptive immunity to SARS-CoV-2 in children in order to define possible immunization strategies and reconsider pandemic control measures. Noteworthy, discussion about quarantine times has been recently fueled by proposals to reduce such measure to 1 week. In the current work we describe for the first time to our knowledge, deep virological (by digital droplets PCR) and immunological (SARS-CoV-2 specific cellular and humoral responses) features of infected children 7 days after symptoms onset. We analyzed anti-SARS-CoV-2 antibodies (Ab) and their neutralizing activity (PRNT) in 42 COVID-19-infected children at the same time point. Individuals with specific humoral responses presented faster virus clearance, and lower viral load associated to a reduced *in vitro* infectivity. We demonstrated that the frequencies of SARS-CoV-2 specific CD4-CD40L+ T-cells and Spike specific B-cells were associated with the anti-SARS-CoV-2 Ab and the magnitude of neutralizing activity.

The present work shed lights on cellular and humoral anti-SARS-CoV-2 responses in children identifying endpoints and biological criteria which may drive future vaccination trials endpoints and quarantine measures policies.

Piazza Sant'Onofrio, 4
00165 Roma
Tel. +39 06 6859 2508/3784
Fax +39 06 6859 2508
e-mail rossi@opbg.net

Bambino Gesù
Ospedale Pediatrico
Istituto di Ricovero e Cura
a Carattere Scientifico
www.ospedalebambinogesu.it

Bambino Gesù
OSPEDALE PEDIATRICO

Università
degli Studi di Roma Tor Vergata

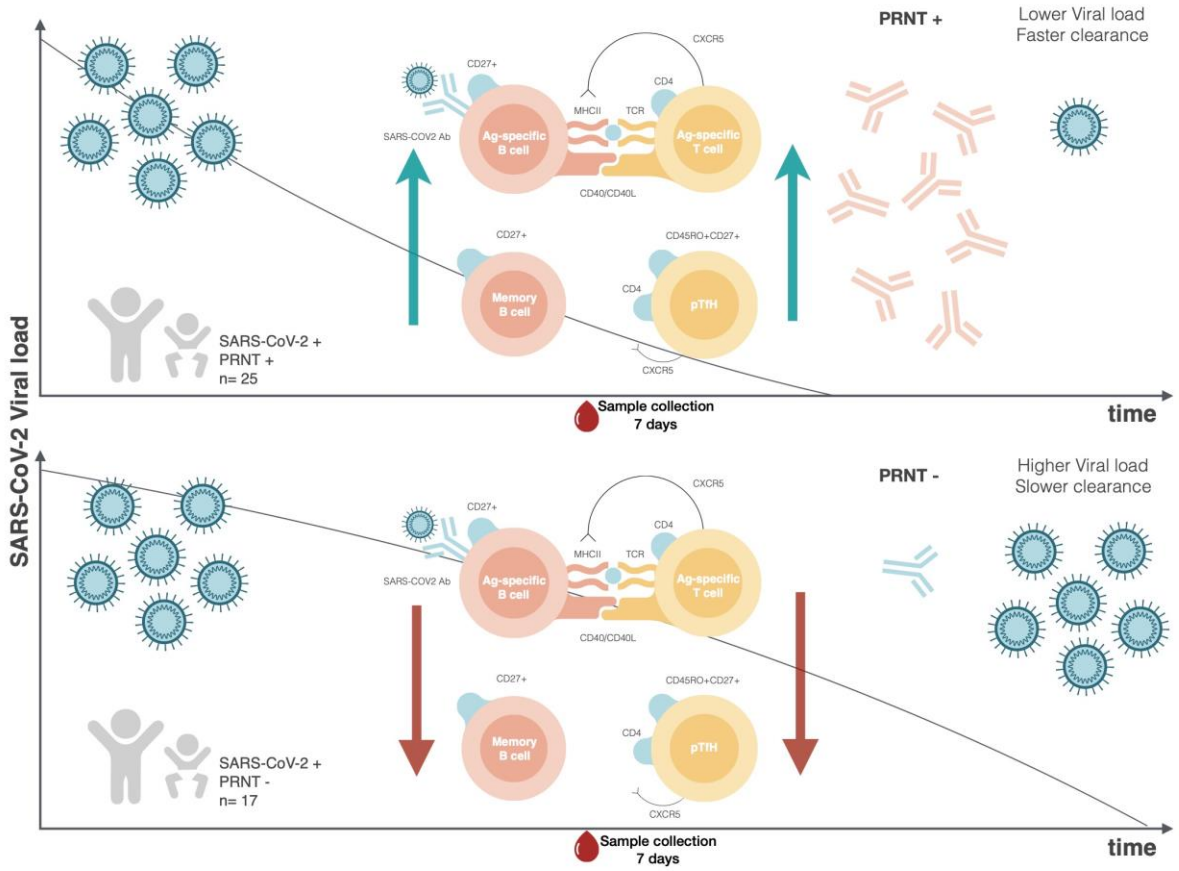

We confirm that the manuscript has never been submitted or accepted for publication elsewhere. All the listed authors have seen and approved the content of the paper and have contributed significantly to the work. We hope you will find this manuscript of interest for your Journal.

Looking forward to your response,

On behalf of the CACTUS study team,

Sincerely,

Paolo Palma, MD, PhD
Head of the Research Unit in Congenital & Perinatal Infections
Academic Department of Pediatrics (DPUO),
Bambino Gesù Children's Hospital-University of Rome “Tor Vergata”,
Rome, Italy

Piazza Sant'Onofrio, 4
00165 Roma
Tel. +39 06 6859 2508/3784
Fax +39 06 6859 2508
e-mail rossi@opbg.net

Bambino Gesù
Ospedale Pediatrico
Istituto di Ricovero e Cura
a Carattere Scientifico
www.ospedalebambinogesu.it

Joint Commission International

Bambino Gesù
OSPEDALE PEDIATRICO

Università
degli Studi di Roma Tor Vergata

paolo.palma@opbg.net

VIROLOGICAL AND IMMUNOLOGICAL FEATURES OF SARS-CoV-2 INFECTED CHILDREN DEVELOPING NEUTRALIZING ANTIBODIES

Authors' list: Nicola Cotugno[1,2,9], Alessandra Ruggiero[1,9], Francesco Bonfante[3,9], Maria Raffaella Petrara[4], Sonia Zicari[1], Giuseppe Rubens Pascucci[1], Paola Zangari[1], Maria Antonietta De Ioris[5], Veronica Santilli[1,5], Emma Manno[1], Donato Amodio[1,2], Alessio Bortolami[3], Matteo Pagliari[3], Carlo Concato[6], Giulia Linardos[6], Andrea Campana[5], Daniele Donà[7], Carlo Giaquinto[7], the CACTUS Study Team, Petter Brodin[8], Paolo Rossi[1,2,10], Anita De Rossi[1,4,10], Paolo Palma[1,2,10].

Affiliations: [1]Academic Department of Pediatrics (DPUO), Research Unit of Congenital and Perinatal Infections, Bambino Gesù Children's Hospital, 00165, Roma, Italy; [2]Chair of Pediatrics, Dept. of Systems Medicine, University of Rome "Tor Vergata", Rome, Italy; [3]Laboratory of Experimental Animal models, Division of Comparative Biomedical Sciences, Istituto Zooprofilattico Sperimentale delle Venezie, 35020, Legnaro, Italy; [4]Section of Oncology and Immunology, Department of Surgery, Oncology and Gastroenterology, Unit of Viral Oncology and AIDS Reference Center, 35128, University of Padova, Padova, Italy; [5]Academic Department of Pediatrics, Bambino Gesù Children's Hospital, IRCCS, Rome, Italy; [6]Department of Laboratories, Division of Virology, Bambino Gesù Children's Hospital, 00165 Rome, Italy; [7]Department of Mother and Child Health, University of Padova, Padova, Italy; [8]Pediatric Rheumatology, Karolinska University Hospital, Sweden.

^ Corresponding author and Lead Contact:

Paolo Palma, MD, PhD,
Head of the Research Unit in Congenital and Perinatal Infections, Academic Department of Pediatrics, Division of Immune and Infectious Diseases
IRCCS Bambino Gesù Children's Hospital
Address: Piazza S. Onofrio, 4- 00165 Rome, Italy
Phone: +390668592455
fax: +390668592508
e-mail: paolo.palma@opbg.net

[9] These authors contributed equally
[10] These authors shared last authorship

SUMMARY

As the global COVID-19 pandemic progresses and with the school reopening, it is paramount to gain knowledge on adaptive immunity to SARS-CoV-2 in children in order to define possible immunization strategies and reconsider pandemic control measures. We analyzed anti-SARS-CoV-2 antibodies (Ab) and their neutralizing activity (PRNT) in 42 COVID-19-infected children 7 days after symptoms onset. Individuals with specific humoral responses presented faster virus clearance, and lower viral load associated to a reduced *in vitro* infectivity. We demonstrated that the frequencies of SARS-CoV-2 specific CD4-CD40L+ T-cells and Spike specific B-cells were associated with the anti-SARS-CoV-2 Ab and the magnitude of neutralizing activity. The plasma proteome confirmed the association between cellular and humoral SARS-CoV-2 immunity, with PRNT+ patients showing higher viral signal transduction molecules (SLAMF1, CD244, CLEC4G). This work shed lights on cellular and humoral anti-SARS-CoV-2 responses in children which may drive future vaccination trials endpoints and quarantine measures policies.

Keywords: SARS-CoV-2; pediatric COVID-19; anti-SARS-CoV-2 antibodies; Ab-mediated neutralization activity; antigen-specific CD4 T cells; antigen-specific B-cells.

Keywords: Total character (including spaces) count is 26,800

INTRODUCTION

The severe acute respiratory syndrome coronavirus 2 (SARS-CoV-2), first emerged in Wuhan in December 2019 (Huang et al., 2020), spread to Europe and in particular to the northern regions of Italy in the beginning of February 2020. On March 11, with more than 100 countries reporting an increasing number of cases, the World Health Organization declared the global pandemic (www.euro.who.int, 2020). Despite the unprecedented scientific effort, the impact of antigen specific cellular immune responses (Altmann & Boyton, 2020), and neutralizing antibodies (Zhang et al., 2020) is only partially known particularly in children. Ab-mediated neutralizing activity was shown 21 days after infection onset in the minority (2 out of 45) of specific monoclonal antibodies isolated from Antigen (Ag) specific B cells (Seydoux et al., 2020) of an infected adult. In particular, the most effective antibody showed a specific binding for the receptor-binding domain (RBD) and was able to prevent viral entry (Seydoux et al., 2020). The contribution of SARS-CoV-2 specific CD4+ T cells to the production of effective neutralizing antibodies has been recently showed in adults (Grifoni et al., 2020; Meckiff et al., 2020; Weiskopf et al., 2020), but no data on its impact on the virus nor its association to Ag specific B cells have been shown.

In the context of pediatric infection, data on the SARS-CoV-2 specific immunity are still scarce. Few studies showed that children are able to develop a robust neutralizing antibody response (Nab) after infection (Liu et al., 2020; Yonker et al., 2020; Zhang et al., 2020). On the other hand, SARS-CoV-2 specific T and B cell immunity needs to be defined in relation to neutralizing antibodies and viral control. Overall children experience milder clinical course of COVID19 as compared to adults (Gupta, Malhotra, Gupta, Agrawal, & Ish, 2020), and it is paramount to define the impact of adaptive SARS-CoV-2 specific immunity on viral spread and clinical course in pediatric cases (Brodin, 2020).

In this work we aim to define the humoral and cellular response in 42 SARS-CoV-2 infected children. We investigated the neutralizing antibodies (Abs) activity in SARS-CoV-2 infected children and its impact on the viral load in nasopharyngeal swabs (NP). We further explored Ag specific T and B cells defined as CD4+CD40L+ and SARS-CoV-2 spike (S1+S2) positive switched B cells. Finally we provided a comprehensive proteomic profile focusing on differences between SARS-CoV-2 infected individuals with differential neutralizing ability.

RESULTS

Clinical and standard laboratory profile of SARS-CoV-2 infected children compared to SARS-CoV-2 neg.

Standard laboratory analysis and demographic characteristics were explored in order to define differences among SARS-CoV-2 infected children (SARS-CoV-2+), and those admitted for the clinical suspicion of SARS-CoV-2 but tested negative by both virological and serological methods (SARS-CoV-2 neg). SARS-CoV-2+ children were investigated for SARS-CoV-2 Ab titers and for the presence of neutralizing Abs measured by plaque reduction neutralization test (PRNT) on samples collected 7 days after symptoms onset. As shown in Table 1, patients were further stratified in PRNT+ and PRNT-, with seventeen (17/42, 40%) SARS-CoV-2 infected children been PRNT-. No significant differences in terms of age, male/female ratio, lymphocytes' count, hemoglobin (Hb) was found between PRNT+ and PRNT- and SARS-CoV-2 neg (Table 1). Higher white blood cell count (WBC) was found in SARS-CoV-2 neg compared to PRNT+ ($p=0.002$) and PRNT- ($p=0.042$). This result is in line with the higher CRP levels found in SARS-CoV2 neg compared to both PRNT+ and PRNT- ($p<0.0001$ and $p=0.001$, respectively, Table 1), supporting an alternative infectious/inflammatory condition in SARS-CoV-2 neg. At admission, PRNT+ and PRNT- patients did not differ with regards to symptomatology, according to WHO classification (https://www.who.int/publications/i/item/clinical-management-of-covid-19) (Table 1 and Supplementary Table 1).

Sars-CoV-2 specific IgG and Ab neutralizing activity associate with faster virus clearance, lower viral load and reduced *in vitro* infectivity.

In NP, we evaluated the viral load by ddPCR and RT-PCR in association with SARS-CoV-2 humoral responses. Our data show an inverse correlation between viral load in NP and both S1/S2 SARS-CoV-2 IgG ($p=0.0005$; rho=-0.69) (Fig. 1a) and PRNT ($p<0.0001$; rho=-0.67) (Fig. 1b). *In vitro* infectivity, measured by foci forming unit (FFU), showed an inverse correlation with both S1/S2 SARS-CoV-2 IgG ($p=0.003$; rho=-0.67) (Fig. 1c) and PRNT ($p=0.023$; rho=-0.46) (Fig. 1d). Longitudinal analysis confirmed the impact of humoral responses on virus clearance. We calculated the area under the curve (AUC) of the viral load from NP collected every 48 hours up to undetectable viral load, and we found an inverse correlation with SARS-CoV-2 Ab ($p=0.031$; rho=-0.54) (Fig. 1e). We further compared the levels of SARS-CoV-2 viral load in seropositive and seronegative individuals. Our results

show a significantly higher viral load in seronegative patients expressed in terms of both S1/S2 SARS-CoV-2 IgG (p=0.003) and PRNT (p=0.0007) (Fig. 1f). Overall these data confirm the role of SARS-CoV-2 specific humoral responses in controlling virus replication, expected infectivity and virus clearance. As previously reported (GeurtsvanKessel et al., 2020), we found S1/S2 SARS-CoV-2 IgG levels to positively correlate with PRNT titers (p=0.0002; rho=0.65) (Supplementary Fig. 1).

SARS-CoV-2 specific B cells positively associates with SARS-CoV-2 specific IgG and PRNT.

The B cell compartment and the frequency of SARS-CoV-2 specific B cells were analyzed by FACS using an in-house fluorescently labelled probe expressing S1+S2 SARS-CoV-2 proteins (gating strategy in Fig. 2a and Supplementary Fig. 2a). We analyzed the SARS-CoV-2 specific IgD-CD27+ switched B cells (Fig. 2a) and we found a positive association with both S1/S2 SARS-CoV-2 IgG (p=0.003; rho=0.54) and PRNT (p=0.008; rho=0.49) (Fig. 2b and 2c respectively). This association was also confirmed when Ag specific B cells were re- analyzed in SARS-CoV2+ children stratified by their serological status. Indeed, a higher frequency of Ag specific B cells was found in seropositive compared to seronegative SARS-CoV-2 children (p=0.001) (Fig. 2d). Despite being not significant (p=0.052) (Fig. 2e) a higher frequency of Ag specific B cells was also found in PRNT+.

We further explored the standard B cell phenotype and we found no differences in terms of total B cells (CD19+CD10- B cells) in PRNT+ compared to PRNT- (Supplementary Fig. 2b). B cell memory compartment analysis, according to the expression of IgD and CD27, showed a higher frequency of switched memory B cells in PRNT+ compared to PRNT- (Supplementary Fig. 2c) despite no differences in age between the groups. According to the expression of CD21 and CD27, a lower frequency of Tissue like memory (TLM) B cells resulted in PRNT+ compared to PRNT- (Supplementary Fig. 2d).

SARS-CoV-2 specific CD4 T cells are positively associated to PRNT

To further characterize the immunological features of patients with differential neutralization activity against SARS-CoV-2, we investigated CD3+CD4+ general phenotype and frequency of SARS-CoV-2 specific CD4 T cells (gating strategy in Fig. 3a and Supplementary Fig. 3a). Antigen specific CD4 T cells were defined through the analysis of CD40L after *in vitro* stimulation with SARS-CoV-2 antigens using a previously validated

methodology (Chattopadhyay, Yu, & Roederer, 2006; Cotugno et al., 2017; Cotugno, Morrocchi, et al., 2020; Cotugno, Zicari, et al., 2020; de Armas et al., 2017). Pairwise correlation analysis showed a positive association between Ag specific T cells and Ab mediated neutralization activity (p=0.039; rho=0.39) (Fig. 3c). Furthermore, PRNT+, revealed a higher frequency of SARS-CoV-2 specific T cells compared to PRNT- (p=0.03, Fig. 3e). No differences in terms of Ag specific T cells emerged in patient with differential SARS-CoV-2 IgG serostatus. Overall these results may suggest that Ag specific T cells may correlate with neutralizing antibodies classes other than IgG such as IgA in turn having an higher correlation with mucosal and tissue resident antibodies (Hsueh, Huang, Chen, Kao, & Yang, 2004).

We also explored the standard T cell phenotype and we could benefit from a cohort of healthy age and gender matched children, examined in the pre COVID-19 era. Whereas no differences emerged in terms of total CD3+CD4+ between PRNT+, PRNT- , and SARS-CoV-2 neg, both SARS-CoV-2 positive groups (PRNT+ and PRNT-) showed an higher CD3+CD4+ frequency compared to HC (p=0.001 and p=0.017 respectively) (Supplementary Fig. 3b). Maturational subsets were analyzed according to the surface expression of CD45RO and CD27. PRNT+ expressed a significantly lower frequency of terminally differentiated effector memory T cells (TEMRA) compared to both PRNT- and SARS-CoV-2 neg patients (Supplementary Fig. 3c). Through the expression of CXCR5 on live CD3+CD4+CD45RO+CD27+ central memory T cells we investigated peripheral follicular T helper cells (pTfH). Our analysis showed a lower frequency of pTfH in both PRNT+ and PRNT- patients compared to HC (p=0.004 and p=0.004 respectively) (Supplementary Fig. 3d). We also found that PRNT- had lower pTfH compared to SARS-CoV-2 neg children (p=0.040) (Supplementary Fig. 3d) suggesting how the frequency of this subset, can play a crucial role in the context of SARS-CoV-2 infection.

Proteomics characteristics of SARS-COV-2 patients with differential neutralizing activity.

We explored plasma proteomic correlates of immune responses in patients with SARS-CoV-2 neutralization activity. We could benefit from previous data generated with Olink platform on plasma samples collected in our cohort at diagnosis, and before treatment initiation (Camila Rosat Consiglio & CACTUS study team, 2020). We obtained 121 unique plasma proteins using two Olink panels associated with inflammation pathways filtering out proteins

with >30% measurements below the threshold of detection. Principal component analysis (PCA) analyzed for proteomics revealed no clear clusters between PRNT+ and PRNT- (data not shown), suggesting a similar pro-inflammatory pattern in both SARS-COV-2 groups which overall resulted similar in terms of symptomatology (see Table 1 and Supplementary Table 1). The full dataset of correlations is available in Supplementary Fig. 4.

We further assessed whether the presence of neutralizing activity was associated with differential expression of specific plasma factors. Two different proteins belonging to the Signaling Lymphocytic Activation Molecule pathway, SLAMF1 (Fig. 4a) and CD244 (Fig. 4b) resulted significantly higher in PRNT+ compared to PRNT- (p=0.002 and p=0.03, respectively). Such molecules were previously showed to be present on activated T and B cells and to be essential receptor and signaling transductors for viral entry (Koethe, Avota, & Schneider-Schaulies, 2012). Proteomic analysis also showed that PRNT+ had higher levels of other two factors associated with signal transduction and viral entry. First, CLEC4G (p= 0.017, Fig 4c) which is a glycan-binding receptor already described to act as recognition and uptake molecule for multiple viruses including SARS coronaviruses (Gramberg et al., 2005). Second, Fc receptor like 6 (FCRL6) (p=0.017, Fig. 4d) which can act as major histocompatibility complex II receptor (MHC II) mediating virus entry (Schreeder et al., 2010). Finally, correlation analysis confirmed that SLAMF1 was positively associated with PRNT (p=0.001, Fig 4e), SARS-CoV-2 IgG (p=0.0003, Fig. 4f) and Ag specific B cells (p=0.028; Supplementary Fig. 5a). These data collectively confirm a close relation between cellular and neutralizing activity in SARS-CoV-2 immunity.

Multiomics Factor Analysis (MOFA) revealing predictors of anti-Sars Cov2 neutralization activity.

In order to provide a comprehensive immunologic description of patients with differential ability to produce neutralizing antibodies, we applied Multiomics Factor Analysis (MOFA) (Argelaguet et al., 2019). In this analysis we used as input: phenotypic features describing T and B cell, Ag specific cells frequencies and plasma proteins. We focused on the top seven factors which were identified as major contributors towards the neutralization activity (Fig. 5a). Among those, the plasma proteome did not show relevant contribution (Factor 1 in Fig. 5a and Supplementary Fig. 6a). Conversely, factors 3 and 6, mainly driven by the frequencies of B and T cell subsets were able to discriminate between PRNT+ and PRNT- (Fig. 5b). This analysis proved that resting memory B cells (IgD-CD27+CD21+) and

activated memory B cells (IgD-CD27+CD21-) in factor 3 (Fig. 5c) along with activated T-Bet+ B cell subsets (Supplementary Fig. 6b) in factor 6 represented the main loading features for the identification of PRNT+/PRNT- groups. For the T cell subsets in factor 3, the highest weight for group discrimination was mainly provided by the frequency of CM, EM and CD40L+ memory T cells (Fig. 5d). Overall these data suggest that the development of neutralizing antibodies is favored by the presence of an intact memory B and T cell compartment

DISCUSSION

This work provides a virological and immunological characterization of SARS-CoV-2 infected children presenting a differential Ab-mediated neutralizing activity. It further shows that children with neutralizing antibodies present reduced viral load, faster virus clearance and lower *in vitro* infectivity. These data provide information that can drive vaccination endpoints and quarantine measures policies. In particular, we explored SARS-CoV-2 specific humoral and cellular responses in PBMCs and plasma collected 1 week after symptoms onset. We correlated such results with quantitative analysis of SARS-CoV-2 viral load and *in vitro* infectivity. We stratified the cohort according to humoral responses and we found that SARS-CoV-2 viral load was lower in individuals with both SARS-CoV-2 IgG and PRNT, showing the impact of Ab mediated responses on SARS-CoV-2 viral load in NP in children. Confirming previous *in vitro* findings (Camila Rosat Consiglio & CACTUS study team, 2020; Walls et al., 2020), we here showed that children presenting higher anti-Spike protein IgG levels and higher concentrations of neutralizing antibodies are the ones with lower viral burdens and faster virus clearance. This information further confirms that pediatric patients are able to mount a humoral response relatively early after symptoms onset (Yonker et al., 2020) which affects both viral load and virus clearance. Although there is yet no consensus that a higher viral load in NP correlates with a higher infectivity of patients, we here show the impact of humoral immunity on virus replication, *in vitro* infectivity and presumably on virus spread. Hence, SARS-CoV-2 infected children able to mount an *in vitro* neutralization could benefit from less restrictive quarantine measures.

Further, we studied SARS-CoV-2 specific cellular responses that are still unknown in the pediatric setting. Indeed, recent works have mainly focused on adult groups and demonstrated a clear association between the presence of SARS-CoV-2 specific CD4+ T cells and the development of effective neutralizing activity (Altmann & Boyton, 2020; Carolyn

Rydyznski Moderbacher, 2020; Grifoni et al., 2020; Weiskopf et al., 2020). In the present study we confirmed a positive association between humoral responses and SARS-CoV-2 specific CD4+ T cells in children. In particular, individuals with elevated levels of SARS-CoV-2 specific CD4+ T cells also showed elevated levels of effective neutralizing activity, associated with reduced viral load. We further revealed that Ag specific B cells were positively associated with SARS-CoV-2 neutralization activity and IgG titers. These results suggest Ag specific B cell frequency as a cellular marker for Ab-mediated neutralization.

We then moved on to explore whether neutralization activity was associated with particular B and T cell phenotype characteristics that could favor humoral responses in SARS-CoV-2 infected children. Present data showed that neutralization activity was associated with lower levels of exhausted B and T cell phenotypes. Indeed, TLM B cell frequencies, previously showed to be higher in chronic infections (Meffre et al., 2016; Moir et al., 2008), resulted lower in PRNT+ patients. Accordingly, memory B cells were positively associated with both SARS-CoV-2 IgG and PRNT titers. These B cell phenotype characteristics can be thus useful to estimate the ability of the patients to produce anti SARS-CoV-2 humoral responses. Of note, these results are in line with recent report in adults showing that the majority (>90%) of Ag specific cells able to produce effective neutralizing antibodies present a memory phenotype (Seydoux et al., 2020). This observation may further support the use of convalescent plasma containing high dose of neutralizing antibodies (Tonn et al., 2020), as previously attempted to support faster virus clearance in critical cases of COVID-19 (NCT04391101, NCT04374370) (Shen et al., 2020; Valk et al., 2020).

The characterization of children with differential anti SARS-CoV-2 neutralizing activity was enriched by the analysis of plasma proteomic profiling. We found that few proteins involved in the viral signal transduction were differentially expressed in PRNT+ and PRNT-. In particular, SLAMF1 and CD244 were significantly higher in PRNT+ patients compared to PRNT-. Such molecules are crucial in activated lymphocytes to transduce the signal of an MHC processed antigen, such as measles virus (Lin & Richardson, 2016). In line with this, few evidence showed the homologous protein domains of measles virus and coronaviruses, including SARS-CoV-2 (Walls et al., 2020). Indeed, it was recently argued that an adaptive protection may be provided by the measles mumps and rubella vaccine and BCG (Mantovani & Netea, 2020; Sidiq, Sabir, Ali, & Kodzius, 2020). Furthermore, CLEC4G, already described to act as recognition and uptake molecule for multiple viruses including

Ebola, West Nile and SARS coronaviruses (Gramberg et al., 2005) was found higher in PRNT+ compared to PRNT-. Overall these data confirm the close relation between cellular and humoral responses to control SARS-CoV-2 burden in children.

This study presents some limitations. First, our study included patients with scarce symptoms variability, thus we were not able to clearly identify differences in terms of both SARS-CoV-2 cellular and humoral responses according to symptomatology. However, it is important to note that asymptomatic patients (n=9) included in our cohort and 11 multi inflammatory syndrome associated to COVID-19 (MIS-C) patients, previously published (Camila Rosat Consiglio & CACTUS study team, 2020), showed no major differences in terms of SARS-CoV-2 serology and neutralization activity compared to mild COVID-19 cases (Camila Rosat Consiglio & CACTUS study team, 2020). This data support the hypothesis that inflammation dynamics rather than adaptive immunity orchestrate the clinical course of the disease and specifically the development of MIS-C. Another limitation is represented by the plasma proteome profiling which was extrapolated from a previous study, due to sample unavailability, and it was focused on systemic inflammation rather than antiviral adaptive immunity. Nonetheless, it is still interesting to note that inflammation markers were not able to discriminate between PRNT+ and PRTN- patients, supporting the hypothesis that the ability to produce neutralizing antibodies does not directly associate with grade of inflammation, but rather with the status of the immune system.

Overall this work provides a description of SARS-CoV-2 specific humoral and cellular immunity in children and its relation to virus load, virus clearance and infectivity. Both antigen specific T and B cells positively correlate with anti-SARS-CoV-2 antibody titers and neutralization activity, suggesting a cell correlates of SARS-CoV-2 immunity in this population. Public health restrictive measures should take into account such results in order to reconsider timing of confinement and NP retesting in pediatric patients presenting strong humoral responses. Additional confirmatory studies involving adult cohorts as well as larger cohorts of children with COVID-19 and with a higher symptom variability are needed.

STAR METHODS

RESOURCE AVAILABILITY

Lead Contact

Further information and requests for resources and reagents should be directed to and will be fulfilled by the Lead Contact, Dr. Paolo Palma (paolo.palma@opbg.net).

Materials Availability

This study did not generate new unique reagents.

Data and Code Availability

The published article includes all dataset generated or analyzed during this study.

The datasets supporting the current study have not been deposited in a public repository because are unpublished, but they will be made available upon paper acceptance.

Study participants and samples collection

Forty two SARS-CoV-2 infected children (SARS-CoV-2 +) and 11 SARS-COV2 negative controls (SARS-CoV-2 neg) were enrolled in the CACTUS (Immunological studies in **C**hildren **A**ffe**CT**ed by covid and ac**U**te re**S**piratory diseases) study from March to April 2020 at Bambino Gesu' Children's Hospital in Rome. Local ethical committee approved the study and written informed consent was obtained from all participants or legal guardians. Age, gender, clinical and routine laboratory characteristics of the cohort are described in Table 1. SARS-CoV-2 + were patients tested positive for SARS-CoV-2 real-time reverse transcriptase–polymerase chain reaction (RT-PCR) tests (GeneXpert, Cepheid, Sunnyvale, CA; 250 copies/mL sensitivity, 100% specificity) in nasopharingeal swab (NP). SARS-CoV-2 + were stratified according to presence (PRNT+) or absence (PRNT-) of neutralizing antibodies. Controls enrolled in the studies (SARS-CoV-2 neg) were children admitted to our hospital with suspected SARS-CoV-2 infection, due to fever or respiratory symptoms, but tested negative for 2 consecutive nasopharyngeal swabs (performed 24 hours apart) and for SARS-CoV-2 S1/S2 IgG test. Longitudinal blood samples were collected at admission, after 48 hours and approximately 7 to 14 days after admission. Viral load in NP was performed in SARS-CoV-2 + every 48 hours up to undetectable viral load.

METHOD DETAILS

Sample collection and storage

Venous blood was collected in EDTA tubes and processed within 2 hours. Plasma was isolated from blood and stored at -80°C. Peripheral blood mononuclear cells (PBMCs) were isolated from blood of all patients with Ficoll density gradient and cryopreserved in FBS 10% DMSO until analysis, in liquid nitrogen. Nasopharyngeal swab preserving media was stored at -80°C until use.

Detection and quantification of SARS-CoV2 RNA in Nasopharyngeal swab (NP). SARS-CoV-2 viral load was evaluated using both RT-PCR and ddPCR. For the RT-PCR, the qualitative SARS-CoV-2 real-time reverse transcriptase–polymerase chain reaction (RT-PCR) tests was used according to manufacturer instruction (Seegene's Allplex 2019-nCoV Assay, Republic of Korea). The assay is designed to allow for detection of both E and RdRp genes, which showed comparable specificity for SARS-CoV-2 (Corman et al., 2020). The system is designed to provide an auto-interpretation of the data alongside a Ct value resulting from the amplification of each gene.

An in-house multiplex quantitative assay based on One-Step RT- digital droplet (dd) PCR was used to quantitate SARS-CoV-2 viral load. Total RNA was isolated from NP preserving media and eluted in a final volume of 100µl. The reaction mixture consisted of 5 ml of supermix (Bio-Rad, CA, USA), 2 µl of reverse transcriptase; 2 µl of DTT final concentration 300mM; forward and reverse primers of SARS-CoV-2 E gene (Corman et al., 2020) to a final concentration of 400 nM each and probe to a final concentration of 200 nM; housekeeping GAPDH was amplified under the same conditions using the GAPDH Kit (PE Applied Biosystems); 5 µl of nucleic acids eluted from nasapharyngeal swab samples into a final volume of 20 µl. Each well of the prepared mix is loaded into the 8-channel cartridge to generate the droplets in the oil suspension according to manufacturer (Bio-Rad). Reverse transcription and PCR cycles were run as follow: at 42-50°C for 60 min; enzyme activation 95°C for 10 min; denaturation of cDNA at 95°C for 30sec and annealing/extension at 60°C for 1 min, this two passages were repeated for 40 cycles; enzyme deactivation at 98°C for 10 min. The droplets were then read by the QX200™ Droplet Reader (Bio-Rad) and the results were analyzed with the QuantaSoft™ Analysis Software 1.7.4.0917 (Bio-Rad). Wells with less than 10000 droplets were discarded from the analysis. GAPDH housekeeping gene

was employed to control for the quality of extracted RNA. Each sample was run at least in duplicate. The final results were expressed as SARS-CoV-2 copies/5 µl. We compared the results obtained by both ddPCR and RT-PCR and we found a significant inverse linear correlation between the Ct values of RT-PCR and the viral copy number provided by the ddPCR (r=-0.906, p<0.0001). The derived formula y=-3.40 x+ 36.88 was employed to convert the Ct values in viral copies for samples tested only by RT-PCR.

AUC

The SARS-CoV-2 viral load measurements for the gene E in NP were used to calculate the AUC as follow. The viral load was calculated at multiple time points to calculate the area under the curve for each patient. The curves were drawn plotting on the y-axis the viral copies and on the x-axis the number of days between the date of swab collection and the date of onset of symptoms for symptomatic patients and the hospital admission date for non-symptomatic ones. The average value was considered for the association with PRNT and SARS-CoV-2 IgG.

Virus titration by focus forming assay (FFA)

Vero E6 cells (ATCC® CRL 1586™) were cultured in Dulbecco's modified Eagle's medium (DMEM, Gibco) supplemented with 10% FBS, penicillin (100 U/ml) and streptomycin (100U/ml), at 37°C in a humidified CO2 incubator. To titrate virus infectivity, nasopharyngeal swab preserving media was filtered through a 0.22 µm filter and serially diluted in DMEM supplemented with 2% FBS, penicillin (100 U/ml) and streptomycin (100U/ml). Dilutions were incubated on confluent monolayers of Vero E6 cells, in 96-well plates, for 1 hour. After infection, the inoculum was removed and an overlay of MEM, 2% FBS, penicillin (100 U/ml) and streptomycin (100U/ml) and 0.8% carboxymethyl cellulose was added. After 27 hours, the overlay medium was removed and cells were fixed in PBS 4% PFA, for 30 minutes at 4°C. Upon removal, cells were permeabilized with a 0.5 % Triton-X-100 solution for 10 minutes. Immunostaining was performed by incubation of the J2 anti-dsRNA monoclonal antibody (1:10,000; Scicons) for 1 hour, followed by incubation with peroxidase-labelled goat anti-mouse antibodies (1:1000; DAKO) for 1 hour and a 7 min incubation with the True Blue™ (KPL) peroxidase substrate. Immuno-reagents were prepared in a solution of 1% BSA and 0.05% Tween-80 in PBS. After each antibody incubation, cells were washed 4 times with a 0.05% Tween-80 PBS solution. Focus forming units per ml (FFU/ml) were

counted after acquisition of pictures at a high resolution of 4800 x 9400dpi, on a flatbed scanner.

Plaque reduction neutralization test (PRNT)

A high- throughput PRNT method was developed *in-house*. Briefly, plasma samples were heat- inactivated by incubation at 56 °C for 30 minutes and 2-fold dilutions were prepared in Dulbecco modified Eagle medium (DMEM). The dilutions were mixed to a 1:1 ratio with a virus solution containing 20-25 FFUs of SARS-CoV-2 and incubated for 1 hour at 37 °C. Fifty microliters of the virus–serum mixtures were added to confluent monolayers of Vero E6 cells, in 96-wells plates and incubated for 1 hour at 37 °C, in a 5% CO_2 incubator. The inoculum was removed and 100 µl of overlay solution of Minimum essential medium (MEM), 2% fetal bovine serum (FBS), penicillin (100 U/ml), streptomycin (100 U/ml) and 0.8% carboxy methyl cellulose was added to each well. After 26 hours' incubation, cells were fixed with a 4% paraformaldehyde (PFA) solution. Visualization of plaques was obtained with an immunocytochemical staining method using an anti-dsRNA monoclonal antibody (J2, 1:10,000; Scicons) for 1 hour, followed by 1-hour incubation with peroxidase-labeled goat anti-mouse antibodies (1:1000; DAKO) and a 7-minute incubation with the True BlueTM (KPL) peroxidase substrate. FFUs were counted as described above. The serum neutralization titer was defined as the reciprocal of the highest dilution resulting in a reduction of the control plaque count >50% ($PRNT_{50}$). We considered a titer of 1:10 as the seropositive threshold.

Generation of Sars-CoV-2 probe to select B-cells antigen specific cells

The S1+S2 Spike SARS-CoV-2 protein was obtained from MyBiosource and labelled with Lightning-Link® R-PE Conjugation Kit (Innova Biosciences) to obtain a SARS-CoV2-R-PE.

Ag-specific B-cells by Flow Cytometry

PBMCs underwent surface staining for the B cell phenotype with the following antibodies: CD10 Pe-Cy7(HI10a) from Biolegend, CD19 APC-R700(SJ25C1), CD21 APC(B-Ly4), CD27 FITC(M-T271), IgD BV421(IA6-2), IgM PE-CF594(G20-127), IgG BV605(G18-145) from BD, S1+S2 Sars-CoV2-R-Phycoerythrin (-R-PE) and Live/Dead (BV510; BD). Following fixing and permeabilization of cells (BD permeabilization solution II 1x), cells were stained with an anti T-bet BV650 (04-46, BD). Cells were acquired using Cytoflex (Beckman Coulter, Brea, CA). Gating strategies are provided in Supplementary Fig 2. Positive cell

gating was set using fluorescence minus one control. Data analyses were performed using Kaluza software (Beckman Coulter).

CD4 Ag-specific T-cells by Flow Cytometry

Thawed PBMC were plated (1.5x10^6/aliquot/200 ul) in 96 well-plate containing CD154-PE (CD40L, BD Pharmingen, Franklin Lakes, NJ, USA), Golgi Stop (SigmaAldrich), anti-CD28 (1µg/ml) and either 0,4µg/ml PepTivator SARS-CoV-2 Prot_S (Milteny Biotech, Bergisch Gladbach, Germany) or media only. Following 16hrs incubation at 37°C/5% CO2, PBMC were centrifuged and stained with LIVE/DEAD fixable NEAR-IR dead cell stain kit (for 633 or 635 nm excitation, ThermoFisher, Waltham, Massachusetts, US) 1ul per 10^6cells/ml for 15 minutes at room temperature (RT), protected by light. Antigen specific CD40L+CD4+ T cells were identified according to the gating strategy showed in Fig. 3a. Preliminary experiments on unstimulated (UN), SARS-CoV-2 stimulated (STIM), or SEB-stimulated (not shown) healthy controls collected in the pre-COVID-19 era were used to set the gate. Following *in vitro* stimulation with SARS-CoV-2 antigens, only SARS-CoV-2 + patients showed increase in CD40L+ T cells demonstrating the antigen-specific cellular response (Supplementary Fig. 3a). Surface staining was performed using the following antibodies: CD3 PE-CF594 (UCHT1), CD4 BV510 (SK3), CD27 V450 (M-T271), CD45RO PE-Cy5 (UCHL1), CD185 BV605 (CXCR5, RF8B2) from BD (USA); CD197 BV786 (CCR7, 3D12), from Biolegend (San Diego, CA, USA). Intra-cytokines staining (ICS) was performed following permeabilization using BD Perm sol II 1X (BD) and included IFNγ FITC, from BD; TNFα AF700 (Mab11), IL-2 PE-Cy7 (MQ1-17H12), IL-21 APC (3A3-N2), from Biolegend. Gating strategy for T cell phenotype is provided in Supplementary Fig. 3.

Serum protein profiling

Serum proteins were analyzed using a multiplex technology based upon proximity-extension assays (Lundberg et al., 2011). Briefly, each kit consisted of a microtiter plate for measuring 92 protein biomarkers in all 88 samples and each well contained 96 pairs of DNA-labeled antibody probes. To minimize inter- and intra-run variation, the data were normalized using both an internal control (extension control) and an interplate control, and then transformed using a pre-determined correction factor. The pre-processed data were provided in the arbitrary unit Normalized Protein Expression (NPX) on a log2 scale and where a high NPX represents high protein concentration.

Statistical analysis

Statistical analyses were performed using GraphPad Prism 8 (GraphPad Software, Inc., San Diego, CA) and R software (version 3.6.2). Statistical significance was set at $P < 0.05$ and the test were two-tailed. All data were analyzed D'Agostino-Pearson to assess normality. For non-parametric or parametric data, median or mean are presented, respectively and Mann-Whitney non-parametric test or T-test were used for the comparisons, as indicated in figure legends. Chi-square test was used for gender analysis. The AUC values were calculated with the MESS package (version 0.5.6) as described above. Spearman's correlation was used to examine the association between features. In correlation heatmaps only statistically significant correlations were shown. Linear univariate regression analysis were performed with the "lm" function (stats R package version 3.6.2). MOFA was performed with the MOFA2 package (version 1.0) in the R statistical environment (Argelaguet et al., 2019). Graphpad Prism 8 software was used for statistical analysis (of the cells type distribution and serological parameters) for demographic and routine laboratory blood tests.

ACKNOWLEDGMENTS

We would like to thank all patients and guardians who participated to the study and all the CACTUS study nurses team of the COVID-19 Center of "Bambino Gesù "Children'Hospital". We also thank Jennifer Faudella for her administrative assistance. This work was made possible by support from Bambino Gesù Children's Hospital ricerca corrente 2020 to NC and ricerca corrente 2019 to PP, by PENTA and by Fondazione Cassa di Risparmio di Padova e Rovigo, Progetti di Ricerca Covid-19 (ADR participant). We also thank Riccardo Truono for providing graphical support.

The CACTUS study team from the Children's Hospital "Bambino Gesù":

Stefania Bernardi MD; Lorenza Romani MD; Paola Pansa MD; Sara Chiurchiu MD; Andrea Finocchi MD,PhD; Caterina Cancrini Md,PhD; Laura Lancella MD; Laura Cursi MD; Maia De Luca MD; Renato Cutrera MD; Libera Sessa, PhD; Elena Morrocchi, PhD; Lorenza Putignani PhD; Francesca Calò Carducci MD; Patrizia D'Argenio MD; Marta Ciofi degli Atti MD; Carmen D'Amore MD.

DECLARATION OF INTERESTS

The authors declare no competing interests.

FIGURE LEGENDS

Fig.1 SARS-CoV2 specific IgG and Ab neutralization activity were inversely associated with viral load, virus clearance and infectivity. Non-parametric Spearman correlation was used in a-e. Non-parametric Mann Whitney test was used in f). ddPCR=digital droplet PCR; FFU= Foci Forming Unit; AUC=area under the curve; NP=nasopharyngeal swab; light purple triangles= SARS-CoV-2 IgG+; light green triangles= SARS-CoV-2 IgG-; light purple solid circle= PRNT+; light green solid circle = PRNT-.

Fig. 2 SARS-CoV-2 specific B cells are positively associated to anti SARS-CoV-2 IgG and Ab neutralization activity. Gating strategy for antigen specific B-cells is shown in panel a). Spearman and Mann-Whitney were used in panels b-c and in d-e, respectively. Light purple triangles= SARS-CoV-2 IgG+; light green triangles= SARS-CoV-2 IgG-; light purple solid circle= PRNT+; light green solid circle = PRNT-.

Fig. 3 SARS-CoV-2 specific CD4 T cells are positively associated to SARS-CoV-2 specific IgG and Ab neutralization activity. Gating strategy for antigen specific T-cells (CD40L+) is shown in panel a): left side panels show CD40L+CD4+ T cells for unstimulated (UN) and stimulated (STIM) samples in a healthy control (HC). Right side panels show same conditions for a SARS-CoV-2 infected patients. Spearman tests were used in panel b and c. Mann-Whitney test was used in panels d and e. Light purple triangles= SARS-CoV-2 IgG+; light green triangles= SARS-CoV-2 IgG-; light purple solid circle= PRNT+; light green solid circle = PRNT-.

Fig.4 Proteomic analysis revealing distinct patterns in patients with differential anti-SARS-CoV-2 Ab neutralization activity. Non-parametric Mann Whitney test was used in panels a-d. Non-parametric Spearman correlation test was used in e-g. Light purple solid circle= PRNT+; light green solid circle = PRNT-; grey solid circle = healthy control (HC).

Fig. 5 Multiomics Factor Analysis (MOFA) showing clusterization factors of patients with Ab neutralization activity. Fraction of variance explained by 7 latent factors is shown in panel a. Samples distributed across the top six latent factors in b. Top contributing features and loading direction (+ and -) for factor 3 in B cells and T-cells populations are shown in panels c and d respectively. RM= resting memory; AM= activated memory; DN=

double negative; TLM= tissue like memory; CM= central memory; EM= effector memory; TEMRA= terminally differentiated effector memory.

REFERENCES

Altmann, D. M., & Boyton, R. J. (2020). SARS-CoV-2 T cell immunity: Specificity, function, durability, and role in protection. *Sci Immunol, 5*(49). doi: 10.1126/sciimmunol.abd6160

Argelaguet, R., Clark, S. J., Mohammed, H., Stapel, L. C., Krueger, C., Kapourani, C. A., . . . Reik, W. (2019). Multi-omics profiling of mouse gastrulation at single-cell resolution. *Nature, 576*(7787), 487-491. doi: 10.1038/s41586-019-1825-8

Brodin, P. (2020). Why is COVID-19 so mild in children? *Acta Paediatr, 109*(6), 1082-1083. doi: 10.1111/apa.15271

Camila Rosat Consiglio, N. C., Fabian Sardh, Christian Pou, Donato Amodio, Lucie Rodriguez, Ziyang Tan, Sonia Zicari, Alessandra Ruggiero, Giuseppe Rubens Pascucci, Veronica Santilli, Tessa Campbell, Yenan Bryceson, Daniel Eriksson, Jun Wang, Alessandra Marchesi, Tadepally Lakshmikanth, Andrea Campana, Alberto Villani, Paolo Rossi, the, & CACTUS study team, N. L., Paolo Palma, Petter Brodin (2020). The Immunology of Multisystem Inflammatory Syndrome in Children with COVID-19. *Cell, In Press Accepted Manuscript*. doi: https://doi.org/10.1016/j.cell.2020.09.016

Carolyn Rydyznski Moderbacher, S. I. R., Jennifer M. Dan, Alba Grifoni, Kathryn M. Hastie, Daniela Weiskopf, Simon Belanger, Robert K. Abbott, Christina Kim, Jinyong Choi, Yu Kato, Eleanor G. Crotty, Cheryl Kim, Stephen A. Rawlings, Jose Mateus, Long Ping Victor Tse, April Frazier, Ralph Baric, Bjoern Peters, Jason Greenbaum, Erica Ollmann Saphire, Davey M. Smith, Alessandro Sette, Shane Crotty. (2020). Antigen-specific adaptive immunity to SARS-CoV-2 in acute COVID-19 andassociations with age and disease severity. *Cell*. doi: https://doi.org/10.1016/j.cell.2020.09.038

Chattopadhyay, P. K., Yu, J., & Roederer, M. (2006). Live-cell assay to detect antigen-specific CD4+ T-cell responses by CD154 expression. *Nat Protoc, 1*(1), 1-6. doi: 10.1038/nprot.2006.1

Corman, V. M., Landt, O., Kaiser, M., Molenkamp, R., Meijer, A., Chu, D. K., . . . Drosten, C. (2020). Detection of 2019 novel coronavirus (2019-nCoV) by real-time RT-PCR. *Euro Surveill, 25*(3). doi: 10.2807/1560-7917.ES.2020.25.3.2000045

Cotugno, N., De Armas, L., Pallikkuth, S., Rinaldi, S., Issac, B., Cagigi, A., . . . Pahwa, S. (2017). Perturbation of B Cell Gene Expression Persists in HIV-Infected Children Despite Effective Antiretroviral Therapy and Predicts H1N1 Response. *Front Immunol, 8*, 1083. doi: 10.3389/fimmu.2017.01083

Cotugno, N., Morrocchi, E., Rinaldi, S., Rocca, S., Pepponi, I., di Cesare, S., . . . Consortium, E. (2020). Early antiretroviral therapy-treated perinatally HIV-infected seronegative children demonstrate distinct long-term persistence of HIV-specific T-cell and B-cell memory. *AIDS, 34*(5), 669-680. doi: 10.1097/QAD.0000000000002485

Cotugno, N., Zicari, S., Morrocchi, E., de Armas, L. R., Pallikkuth, S., Rinaldi, S., . . . Palma, P. (2020). Higher PIK3C2B gene expression of H1N1+ specific B-cells is associated with lower H1N1 immunogenicity after trivalent influenza vaccination in HIV infected children. *Clin Immunol, 215*, 108440. doi: 10.1016/j.clim.2020.108440

de Armas, L. R., Cotugno, N., Pallikkuth, S., Pan, L., Rinaldi, S., Sanchez, M. C., . . . Pahwa, S. (2017). Induction of IL21 in Peripheral T Follicular Helper Cells Is an Indicator of Influenza Vaccine Response in a Previously Vaccinated HIV-Infected Pediatric Cohort. *J Immunol, 198*(5), 1995-2005. doi: 10.4049/jimmunol.1601425

GeurtsvanKessel, C. H., Okba, N. M. A., Igloi, Z., Bogers, S., Embregts, C. W. E., Laksono, B. M., . . . Koopmans, M. (2020). An evaluation of COVID-19 serological assays informs future

diagnostics and exposure assessment. *Nat Commun, 11*(1), 3436. doi: 10.1038/s41467-020-17317-y

Gramberg, T., Hofmann, H., Moller, P., Lalor, P. F., Marzi, A., Geier, M., . . . Pohlmann, S. (2005). LSECtin interacts with filovirus glycoproteins and the spike protein of SARS coronavirus. *Virology, 340*(2), 224-236. doi: 10.1016/j.virol.2005.06.026

Grifoni, A., Weiskopf, D., Ramirez, S. I., Mateus, J., Dan, J. M., Moderbacher, C. R., . . . Sette, A. (2020). Targets of T Cell Responses to SARS-CoV-2 Coronavirus in Humans with COVID-19 Disease and Unexposed Individuals. *Cell, 181*(7), 1489-1501 e1415. doi: 10.1016/j.cell.2020.05.015

Gupta, S., Malhotra, N., Gupta, N., Agrawal, S., & Ish, P. (2020). The curious case of coronavirus disease 2019 (COVID-19) in children. *J Pediatr, 222*, 258-259. doi: 10.1016/j.jpeds.2020.04.062

Hsueh, P. R., Huang, L. M., Chen, P. J., Kao, C. L., & Yang, P. C. (2004). Chronological evolution of IgM, IgA, IgG and neutralisation antibodies after infection with SARS-associated coronavirus. *Clin Microbiol Infect, 10*(12), 1062-1066. doi: 10.1111/j.1469-0691.2004.01009.x

Huang, C., Wang, Y., Li, X., Ren, L., Zhao, J., Hu, Y., . . . Cao, B. (2020). Clinical features of patients infected with 2019 novel coronavirus in Wuhan, China. *Lancet, 395*(10223), 497-506. doi: 10.1016/S0140-6736(20)30183-5

Koethe, S., Avota, E., & Schneider-Schaulies, S. (2012). Measles virus transmission from dendritic cells to T cells: formation of synapse-like interfaces concentrating viral and cellular components. *J Virol, 86*(18), 9773-9781. doi: 10.1128/JVI.00458-12

Lin, L. T., & Richardson, C. D. (2016). The Host Cell Receptors for Measles Virus and Their Interaction with the Viral Hemagglutinin (H) Protein. *Viruses, 8*(9). doi: 10.3390/v8090250

Liu, P., Cai, J., Jia, R., Xia, S., Wang, X., Cao, L., . . . Xu, J. (2020). Dynamic surveillance of SARS-CoV-2 shedding and neutralizing antibody in children with COVID-19. *Emerg Microbes Infect, 9*(1), 1254-1258. doi: 10.1080/22221751.2020.1772677

Mantovani, A., & Netea, M. G. (2020). Trained Innate Immunity, Epigenetics, and Covid-19. *N Engl J Med, 383*(11), 1078-1080. doi: 10.1056/NEJMcibr2011679

Meckiff, B. J., Ramirez-Suastegui, C., Fajardo, V., Chee, S. J., Kusnadi, A., Simon, H., . . . Vijayanand, P. (2020). Single-cell transcriptomic analysis of SARS-CoV-2 reactive CD4 (+) T cells. *bioRxiv*. doi: 10.1101/2020.06.12.148916

Meffre, E., Louie, A., Bannock, J., Kim, L. J., Ho, J., Frear, C. C., . . . Moir, S. (2016). Maturational characteristics of HIV-specific antibodies in viremic individuals. *JCI Insight, 1*(3). doi: 10.1172/jci.insight.84610

Moir, S., Ho, J., Malaspina, A., Wang, W., DiPoto, A. C., O'Shea, M. A., . . . Fauci, A. S. (2008). Evidence for HIV-associated B cell exhaustion in a dysfunctional memory B cell compartment in HIV-infected viremic individuals. *J Exp Med, 205*(8), 1797-1805. doi: 10.1084/jem.20072683

Schreeder, D. M., Cannon, J. P., Wu, J., Li, R., Shakhmatov, M. A., & Davis, R. S. (2010). Cutting edge: FcR-like 6 is an MHC class II receptor. *J Immunol, 185*(1), 23-27. doi: 10.4049/jimmunol.1000832

Seydoux, E., Homad, L. J., MacCamy, A. J., Parks, K. R., Hurlburt, N. K., Jennewein, M. F., . . . Stamatatos, L. (2020). Analysis of a SARS-CoV-2-Infected Individual Reveals Development of Potent Neutralizing Antibodies with Limited Somatic Mutation. *Immunity, 53*(1), 98-105 e105. doi: 10.1016/j.immuni.2020.06.001

Shen, C., Wang, Z., Zhao, F., Yang, Y., Li, J., Yuan, J., . . . Liu, L. (2020). Treatment of 5 Critically Ill Patients With COVID-19 With Convalescent Plasma. *JAMA, 323*(16), 1582-1589. doi: 10.1001/jama.2020.4783

Sidiq, K. R., Sabir, D. K., Ali, S. M., & Kodzius, R. (2020). Does Early Childhood Vaccination Protect Against COVID-19? *Front Mol Biosci, 7*, 120. doi: 10.3389/fmolb.2020.00120

672 Tonn, T., Corman, V. M., Johnsen, M., Richter, A., Rodionov, R. N., Drosten, C., & Bornstein, S. R.
673 (2020). Stability and neutralising capacity of SARS-CoV-2-specific antibodies in
674 convalescent plasma. *Lancet Microbe, 1*(2), e63. doi: 10.1016/S2666-5247(20)30037-9
675 Valk, S. J., Piechotta, V., Chai, K. L., Doree, C., Monsef, I., Wood, E. M., . . . Skoetz, N. (2020).
676 Convalescent plasma or hyperimmune immunoglobulin for people with COVID-19: a rapid
677 review. *Cochrane Database Syst Rev, 5*, CD013600. doi: 10.1002/14651858.CD013600
678 Walls, A. C., Park, Y. J., Tortorici, M. A., Wall, A., McGuire, A. T., & Veesler, D. (2020). Structure,
679 Function, and Antigenicity of the SARS-CoV-2 Spike Glycoprotein. *Cell, 181*(2), 281-292
680 e286. doi: 10.1016/j.cell.2020.02.058
681 Weiskopf, D., Schmitz, K. S., Raadsen, M. P., Grifoni, A., Okba, N. M. A., Endeman, H., . . . de
682 Vries, R. D. (2020). Phenotype and kinetics of SARS-CoV-2-specific T cells in COVID-19
683 patients with acute respiratory distress syndrome. *Sci Immunol, 5*(48). doi:
684 10.1126/sciimmunol.abd2071
685 www.euro.who.int. (2020). WHO announces COVID-19 outbreak a pandemic [Press release]
686 Yonker, L. M., Neilan, A. M., Bartsch, Y., Patel, A. B., Regan, J., Arya, P., . . . Fasano, A. (2020).
687 Pediatric SARS-CoV-2: Clinical Presentation, Infectivity, and Immune Responses. *J Pediatr*.
688 doi: 10.1016/j.jpeds.2020.08.037
689 Zhang, Y., Xu, J., Jia, R., Yi, C., Gu, W., Liu, P., . . . Sun, B. (2020). Protective humoral immunity
690 in SARS-CoV-2 infected pediatric patients. *Cell Mol Immunol, 17*(7), 768-770. doi:
691 10.1038/s41423-020-0438-3
692

KEY RESOURCES TABLE

REAGENT or RESOURCE	SOURCE	IDENTIFIER
Antibodies		
CD154-PE (CD40L, clone TRP1)	BD	Cat#555700
CD3PE-CF594 (clone UCHT1)	BD	Cat#562280
CD4 BV510 (SK3)	BD	Cat#562970
CD27 V450 (M-T271)	BD	Cat#561408
CD45RO PE-Cy5 (UCHL1)	Biolegend	Cat#304208
CD185 BV605 (CXCR5, RF8B2)	BD	Cat#740379
CD197 BV786 (CCR7, 3D12)	Biolegend	Cat#563710
IL-21 APC (3A3-N2)	Biolegend	Cat#513008
IL-2 PE-Cy7 (MQ1-17H12)	Biolegend	Cat#500326
IFNγ FITC	BD	Cat#552887
IL-2 PE-Cy7 (MQ1-17H12)	Biolegend	Cat#500326
TNFα AF700 (Mab11)	Biolegend	Cat#502928
CD10 Pe-Cy7(HI10a)	Biolegend	Cat#312214
CD19 APC-R700(SJ25C1)	BD	Cat#659121
CD21 APC (B-Ly4)	BD	Cat#559867
CD27 FITC(M-T271)	BD	Cat#555440
IgD BV421(IA6-2)	BD	Cat#565940
IgM PE-CF594(G20-127)	BD	Cat#562539
IgG BV605(G18-145)	BD	Cat#563246
T-bet BV650 (04-46)	BD	Cat#564142
Double Strand RNA (dsRNA J2)	Scicons	J2 produced in mouse
Peroxidase-labeled goat anti-mouse	Thermofisher	Cat#G-21040
True Blue™ (KPL)	SeraCare	Cat#5510-0052
Bacterial and Virus Strains		
Biological Samples		
Peripheral venous EDTA blood	OPBG	n.a.
Swab-preserving media	OPBG	n.a.
Chemicals, Peptides, and Recombinant Proteins		
BD FACS Permeabilizing Solution 2	BD	Cat# 347692
BD Golgi Stop	BD Biosciences	Cat#554724
Anti-CD28 (1µg/ml)	BD	Cat#555725
Bovine Albumin Fraction V (7.5% solution)	Thermofisher	Cat#15260037
Dimethyl sulfoxide	Sigma-Aldrich	Cat#D8418
Dulbecco's Phosphate buffered saline	EuroClone	Cat#ECB4004L
Fetal Bovine Serum	Gibco	Cat#10270-106
Ficoll-Paque PLUS	GE Healthcare	Cat#17-1440-03
PepTivator SARS-CoV-2 Prot_S	Miltenyi Biotec	Cat#130-126-700
S1+S1 SARS-CoV-2 Prot S	Sino Biological	Cat# 40589-V08B1
RPMI 1640	EuroClone	Cat#ECM9106L

Dulbecco's modified Eagle's medium	Gibco	Cat#11995065
Triton-X-100	Sigma	Cat# T8787
Penicillin-Streptomycin	Thermofisher	Cat# 15140122
Paraformaldehyde (PFA) 4% solution	Sigma	Cat# 1004968350
Carbo xymethyl cellulose salt	Sigma	Cat# C5013-500G
MEM	Thermofisher	Cat# 11095080
Tween-80	Sigma	Cat#P1754
Critical Commercial Assays		
Live/dead Fixable Near-IR Dead cell Stain kit	Invitrogen	Cat#L34976
Lightning-Link® R-PE Conjugation Kit	(Innova Biosciences)	Cat#703-0030
Deposited Data		
Experimental Models: Cell Lines		
Vero E6 cells	ATCC	CRL 1586
Experimental Models: Organisms/Strains		
n.a.		
Oligonucleotides		
Primers for SARS-CoV-2 E gene: forward ACAGGTACGTTAATAGTTAATAGCGT	Corman et al, 2020	N/A
Primers for SARS-CoV-2 E gene: reverse ATATTGCAGCAGTACGCACACA	Corman et al, 2020	N/A
Probe: FAM-ACACTAGCCATCCTTACTGCGCTTCG-BBQ	Corman et al, 2020	N/A
Housekeeping GAPDH	PE Applied Biosystems	Cat#402869
GAPDH Kit (PE Applied Biosystems)		
Recombinant DNA		
n.a.		
Software and Algorithms		
Kaluza software	Beckman Coulter	https://www.beckman.com/flow-cytometry/software/kaluza?country=US
R software (v 3.6.2)	R Foundation	https://www.r-project.org/
QuantaSoftTM Analysis Software 1.7.4.0917	Bio-Rad	Cat#1864011

Other		
Droplet Generation Oil for Probes	Bio-Rad	Cat#1863005
One-Step RT-ddPCR Adv Kit	Bio-Rad	Cat#1864022
QX200TM Droplet Generator	Bio-Rad	Cat#1864002
96 well plate	Bio-Rad	Cat#HSS9641
Eppendorf Mastercycler	Eppendorf	Cat#6313000018
QX200TM Droplet Reader	Bio-Rad	Cat#1864003
DG8™ Cartridges	Bio-Rad	Cat#1864008

Table 1

	SARS-CoV-2 + (n= 42)		*SARS-CoV-2 neg*	p value
	PRNT+ (n= 25)	**PRNT- (n= 17)**	**(n= 11)**	
Age (years)	8.6 (3.9-15.7)	1.9 (0.2-14.9)	5.3 (2.1-7.9)	n.s
Male N (%)	16/25 (64)	6/17 (35)	5/11 (45)	n.s.
Platelets (10^3/uL)	238 (200.5-287.8)	269 (199.5-364.5)	324.0 (231.0-525.0)	PRNT+ vs SARS-CoV-2 neg p=0.022
WBC count (10^3/uL)	5.4 (4.3-6.5)	5.6 (4.6-8.5)	8.4 (7.4-10.5)	PRNT+ vs SARS-CoV-2 neg p=0.002 PRNT- vs SARS-CoV-2 neg p=0.042
Neutrophils (10^3/uL)	2.2 (1.8-3.8)	2.6 (1.7-3.9)	4.3 (2.4-6.0)	PRNT+ vs SARS-CoV-2 neg p=0.029
Lymphocytes (10^3/microL)	2.3 (1.9-3.3)	3.0 (1.3-5.3)	3.4 (2.3-4.2)	n.s.
Hb (g/dL)	12.9 (12.1-14.0)	12.1 (11.7-13.7)	12.3 (10.8-12.8)	n.s.
CRP (mg/dL)	0.08 (0.04-0.60)	0.10 (0.04-0.55)	3.4 (2.0-12.08)	PRNT+ vs SARS-CoV-2 neg p<0.0001; PRNT- vs SARS-CoV-2 neg p=0.001
Duration of symptoms at analysis* mean (SD)	8.1 (4.2), n=23	6.4 (2.4), n=15	n.a.	n.s.
Symptoms (0/1/2)	(6/15/4)	(3/10/4)	n.a.	n.s.

Table 1. Continuous data were presented as median and interquartile range (IQR). T test and Mann Whitney test were used for comparison between parametric and not parametric data respectively. Symptomatology: 0= asymptomatic; 1=mild ; 2=moderate according to WHO classification (https://www.who.int/publications/i/item/clinical-management-of-covid-19). * "Duration of symptoms" was calculated as the number of days between symptoms onset and date of analysis; for asymptomatic patients, the symptom onset of the family member or direct contact who resulted positive for SARS-CoOV-2 was used. SD=standard deviation.

Fig. 1

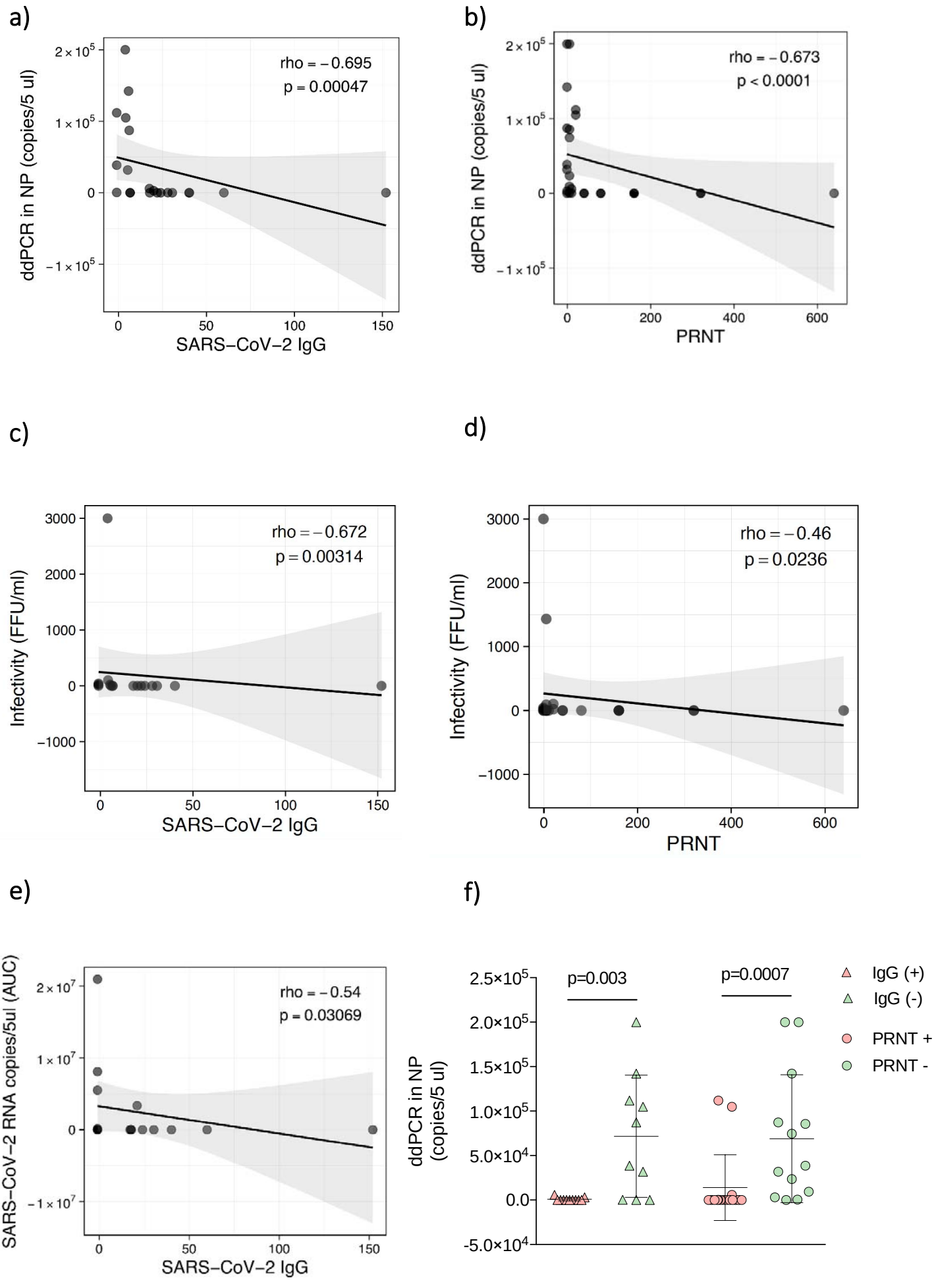
a)
rho = −0.695
p = 0.00047
ddPCR in NP (copies/5 ul)
SARS−CoV−2 IgG
b)
rho = −0.673
p < 0.0001
ddPCR in NP (copies/5 ul)
PRNT
c)
rho = −0.672
p = 0.00314
Infectivity (FFU/ml)
SARS−CoV−2 IgG
d)
rho = −0.46
p = 0.0236
Infectivity (FFU/ml)
PRNT
e)
rho = −0.54
p = 0.03069
SARS−CoV−2 RNA copies/5ul (AUC)
SARS−CoV−2 IgG
f)
p=0.003
p=0.0007
ddPCR in NP (copies/5 ul)
IgG (+)
IgG (-)
PRNT +
PRNT -

Fig. 2

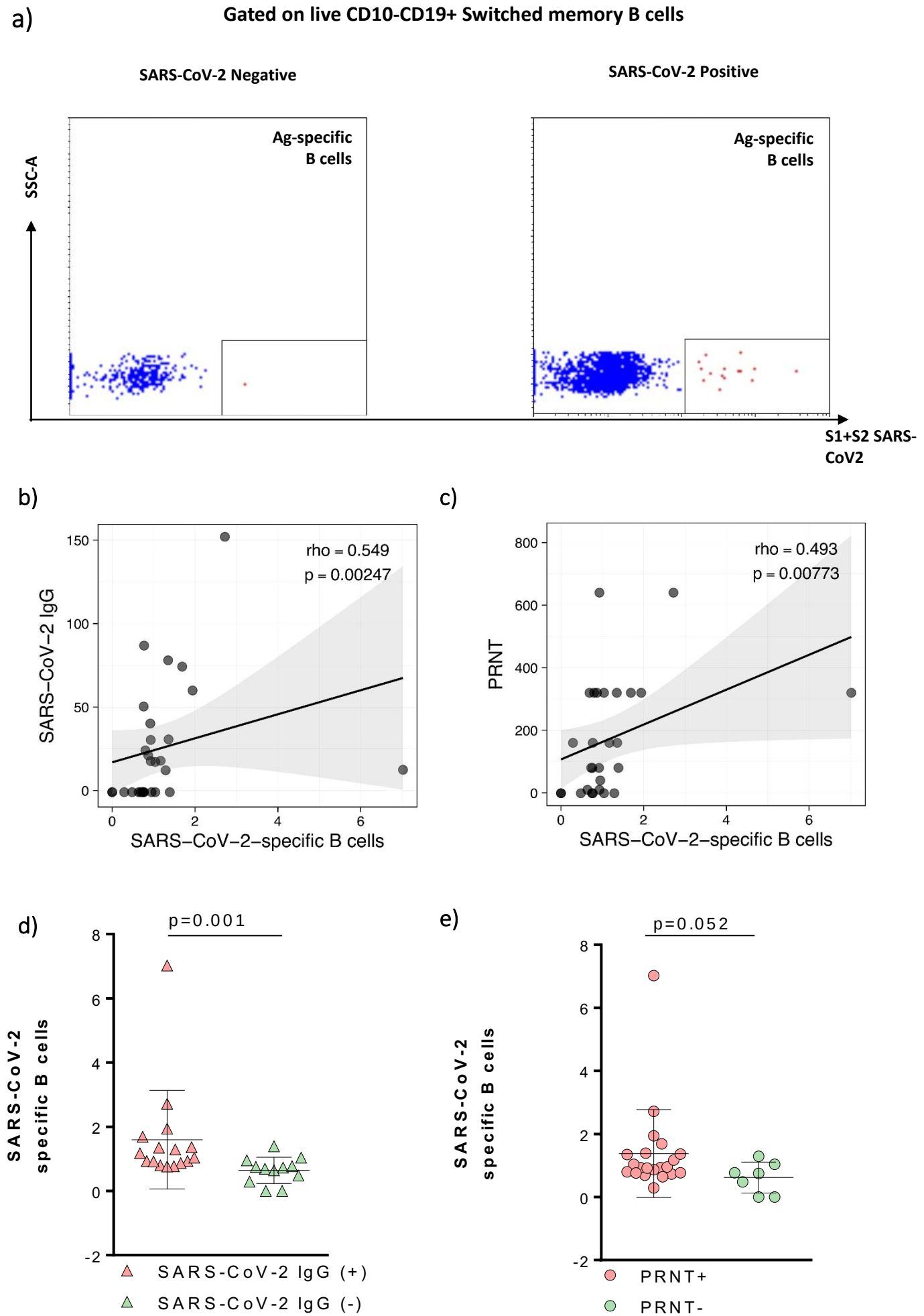
a)
Gated on live CD10-CD19+ Switched memory B cells
SARS-CoV-2 Negative
SARS-CoV-2 Positive
Ag-specific B cells
Ag-specific B cells
SSC-A
S1+S2 SARS-CoV2
b)
rho = 0.549
p = 0.00247
SARS–CoV–2 IgG
SARS–CoV–2–specific B cells
c)
rho = 0.493
p = 0.00773
PRNT
SARS–CoV–2–specific B cells
d)
p=0.001
SARS-CoV-2 specific B cells
SARS-CoV-2 IgG (+)
SARS-CoV-2 IgG (-)
e)
p=0.052
SARS-CoV-2 specific B cells
PRNT+
PRNT-

Fig. 3

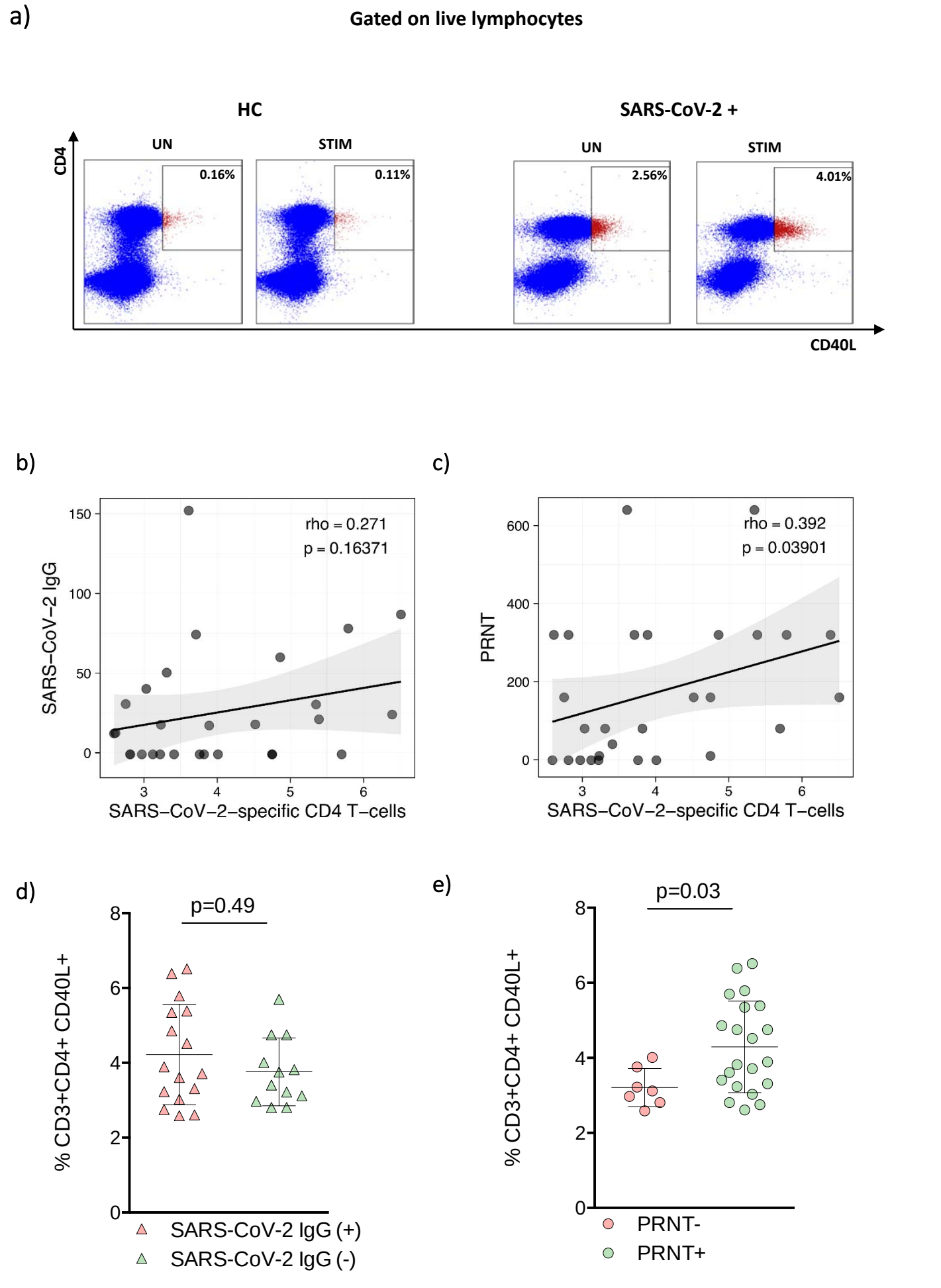
a)
Gated on live lymphocytes
HC
SARS-CoV-2 +
UN
STIM
UN
STIM
CD4
0.16%
0.11%
2.56%
4.01%
CD40L
b)
rho = 0.271
p = 0.16371
SARS–CoV–2 IgG
SARS–CoV–2–specific CD4 T–cells
c)
rho = 0.392
p = 0.03901
PRNT
SARS–CoV–2–specific CD4 T–cells
d)
p=0.49
% CD3+CD4+ CD40L+
SARS-CoV-2 IgG (+)
SARS-CoV-2 IgG (-)
e)
p=0.03
% CD3+CD4+ CD40L+
PRNT-
PRNT+

Fig. 4

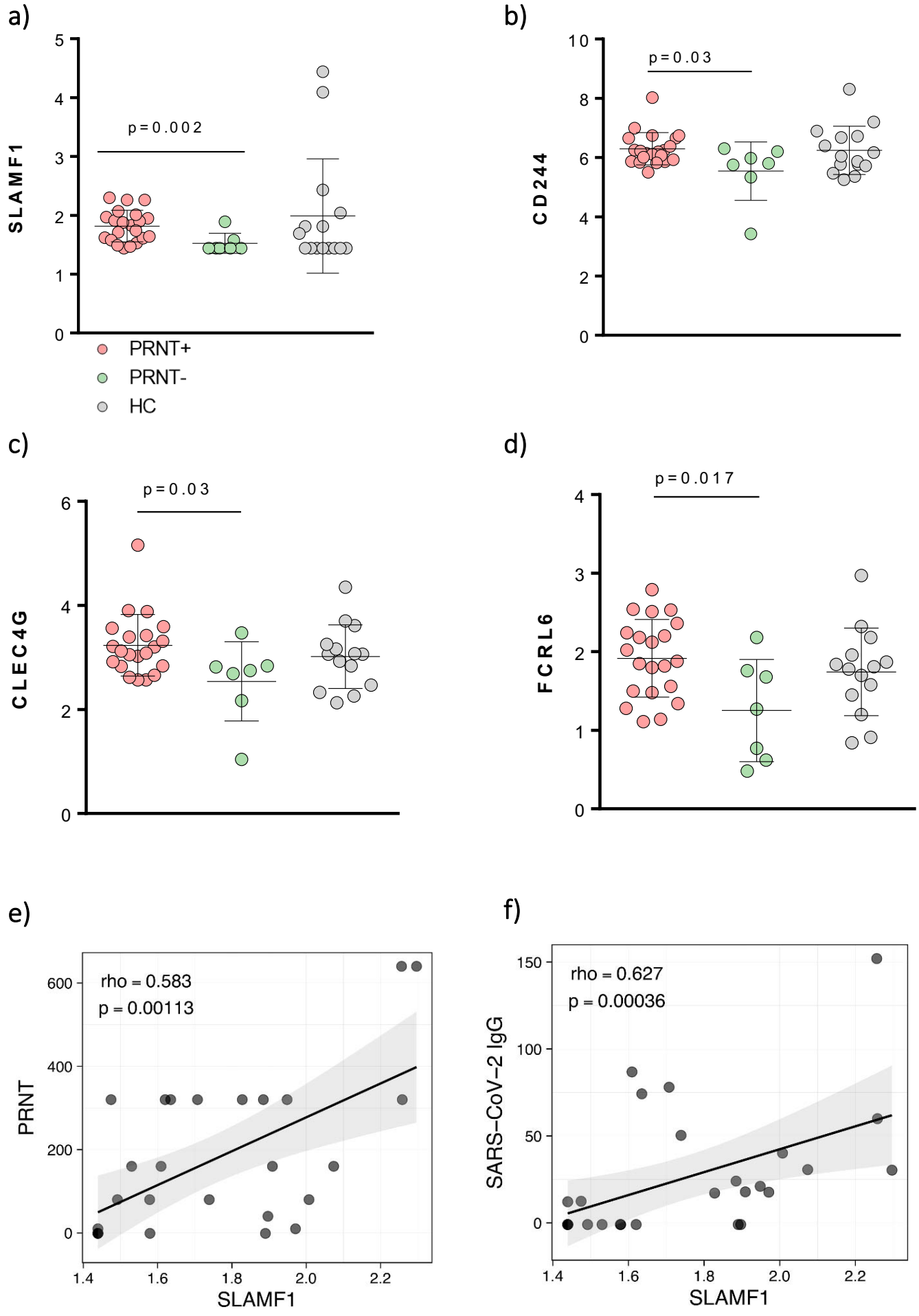
a)
SLAMF1
p = 0.002
PRNT+
PRNT-
HC
b)
CD244
p = 0.03
c)
CLEC4G
p = 0.03
d)
FCRL6
p = 0.017
e)
PRNT
rho = 0.583
p = 0.00113
SLAMF1
f)
SARS–CoV–2 IgG
rho = 0.627
p = 0.00036
SLAMF1

Fig. 5

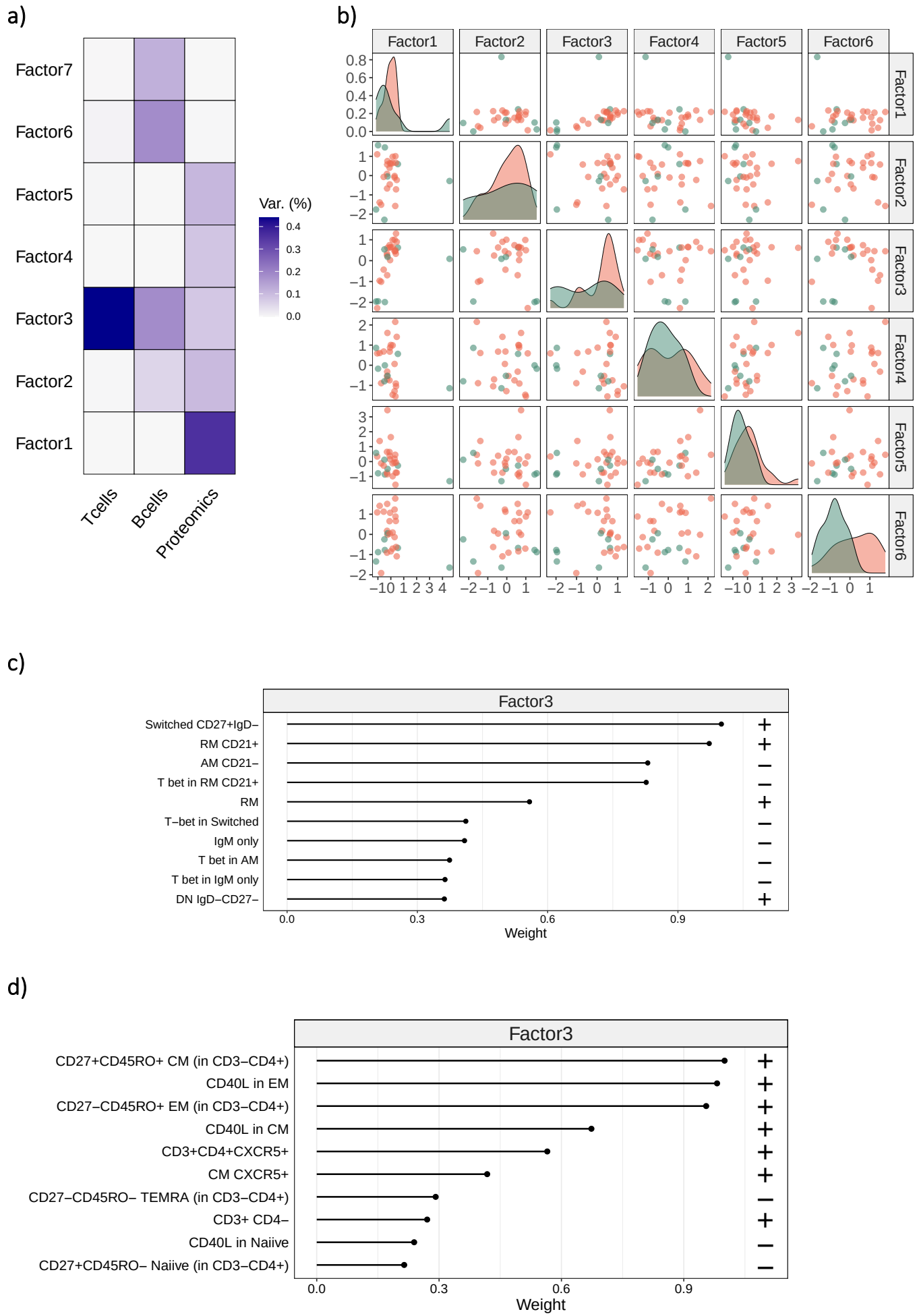
a)
Factor7
Factor6
Factor5
Factor4
Factor3
Factor2
Factor1
Tcells
Bcells
Proteomics
Var. (%)
0.4
0.3
0.2
0.1
0.0
b)
Factor1
Factor2
Factor3
Factor4
Factor5
Factor6
c)
Factor3
Switched CD27+IgD−
RM CD21+
AM CD21−
T bet in RM CD21+
RM
T−bet in Switched
IgM only
T bet in AM
T bet in IgM only
DN IgD−CD27−
0.0
0.3
0.6
0.9
Weight
d)
Factor3
CD27+CD45RO+ CM (in CD3−CD4+)
CD40L in EM
CD27−CD45RO+ EM (in CD3−CD4+)
CD40L in CM
CD3+CD4+CXCR5+
CM CXCR5+
CD27−CD45RO− TEMRA (in CD3−CD4+)
CD3+ CD4−
CD40L in Naiive
CD27+CD45RO− Naiive (in CD3−CD4+)
0.0
0.3
0.6
0.9
Weight

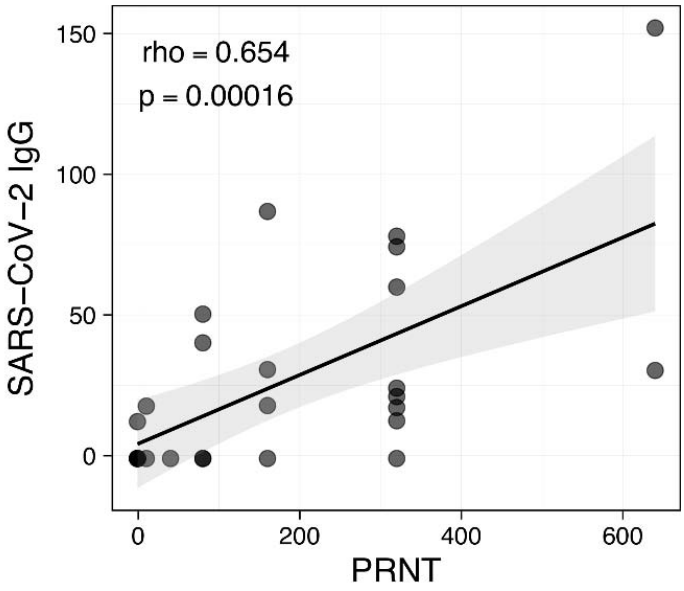

Supplementary Fig. 1 SARS-CoV-2 IgG associates with neutralization activity (PRNT).

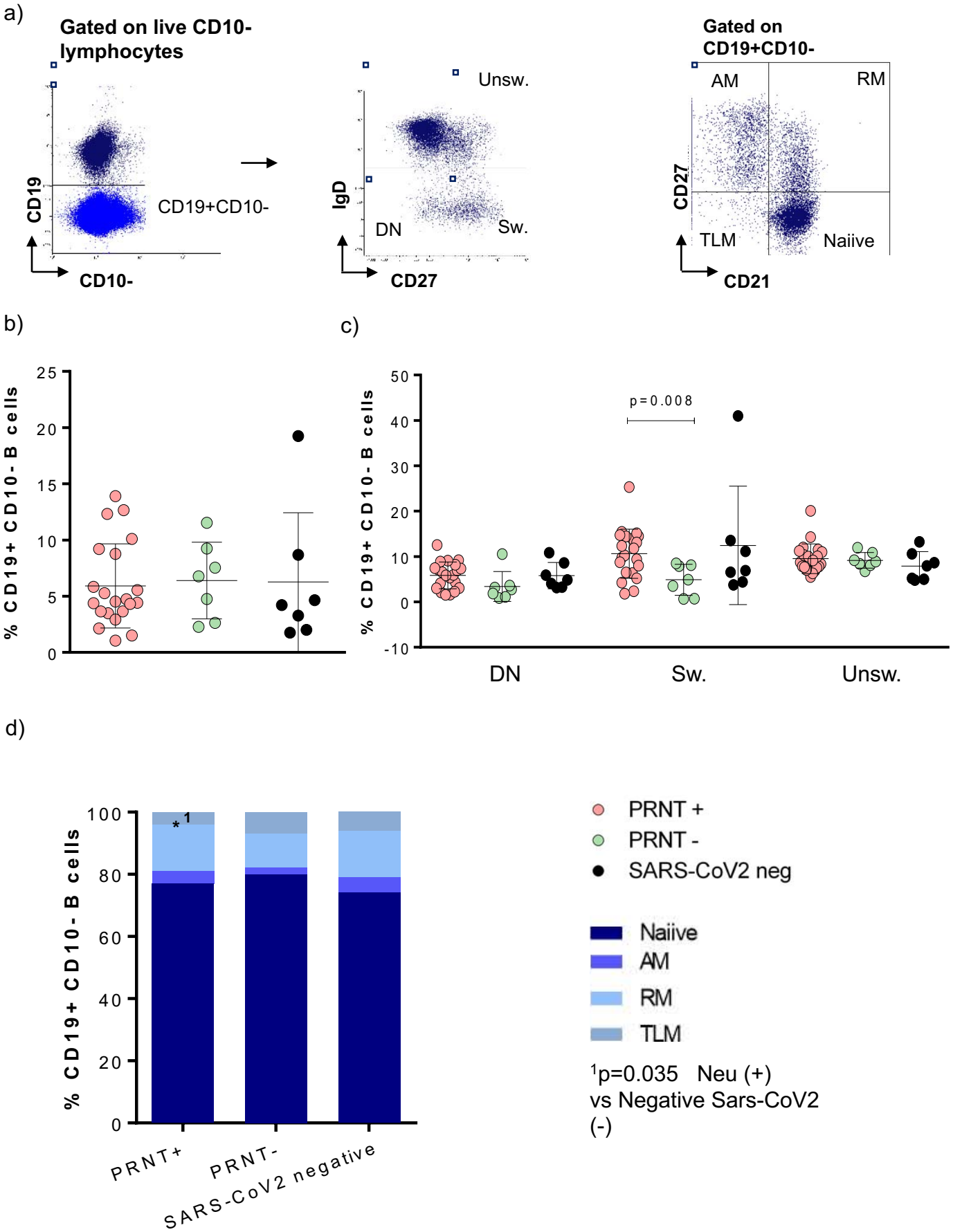

Supplementary Fig. 2 B cells phenotype. Gating strategy for B-cells phenotype is shown in panel a. B cell populations were analyzed in PRNT (+, light purple solid circle), PRNT (-, light green solid circle) and SARS-CoV-2 neg (black solid circle) using non-parametric Mann Whitney test b), c), d). Unsw.: unswitched CD27+IgD+ B cells; Sw.: switched CD27+IgD- B cells AM=activated memory; RM= resting memory; TLM= tissue like memory. Light purple solid circle= PRNT+; light green solid circle = PRNT-; black solid circle = SARS-CoV-2 negative (neg).

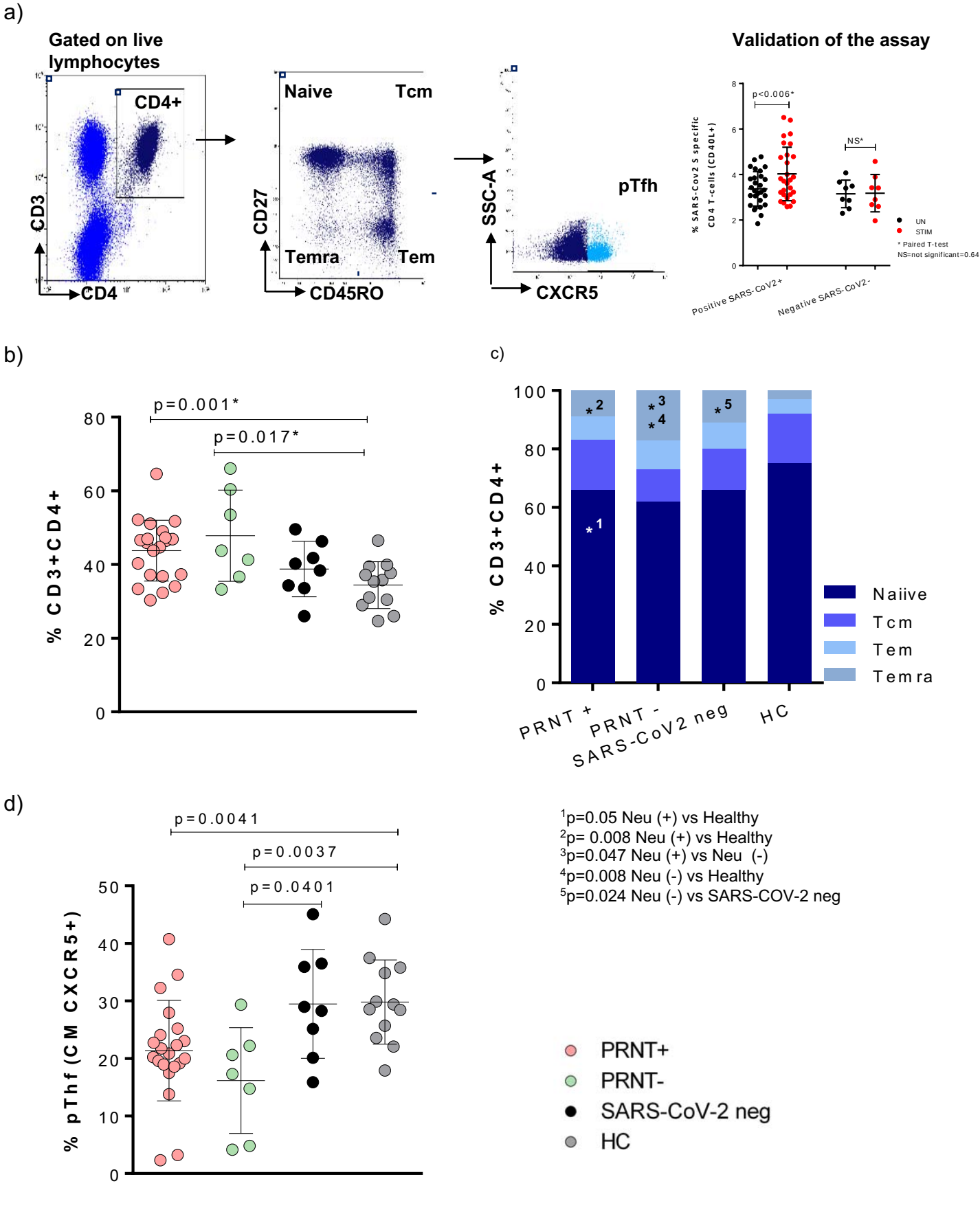

Supplementary Fig. 3 CD4 T-cells phenotype. Gating strategy for T-cells phenotype is shown in panel a. Assay validation is shown in b. T-cell populations were analyzed in PRNT (+, light purple solid circle), PRNT (-, light green solid circle) and SARS-CoV-2 neg (black solid circle) using non-parametric Mann Whitney test c-e. Tcm= central memory; Tem=effector memory; Temra= terminally differentiated effector memory. UN=unstimulated, STIM= SARS-CoV-2 stimulated T-cells

Supplementary Fig. 4 attached separately for higher resolution

Supplementary Fig. 4 Full set of correlation between Ag-specific B and T cells, humoral responses, viral data and proteomics. Only significant correlations are shown in the heatmap.

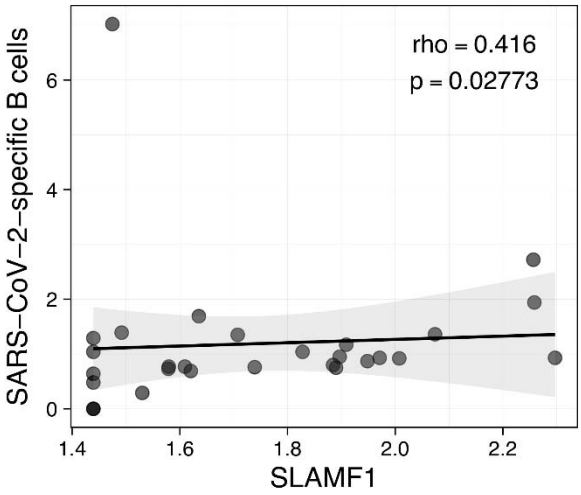

Supplementary Fig. 5 SLAMF1 associates with Ag-specific B cell frequency.

a)

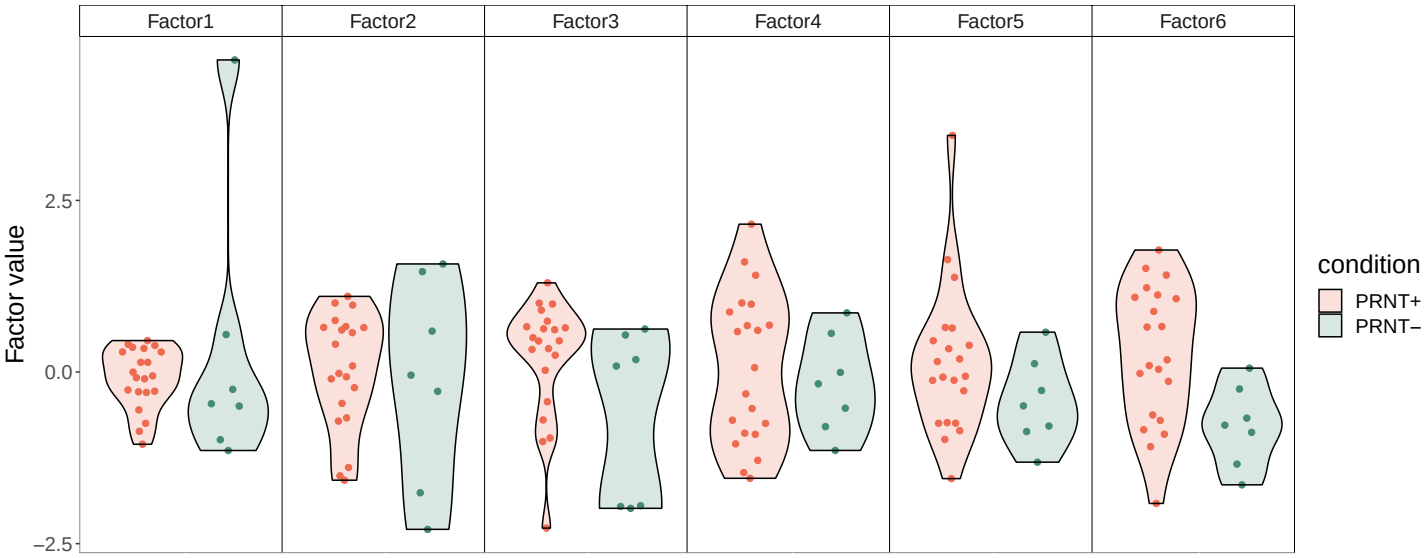

b)

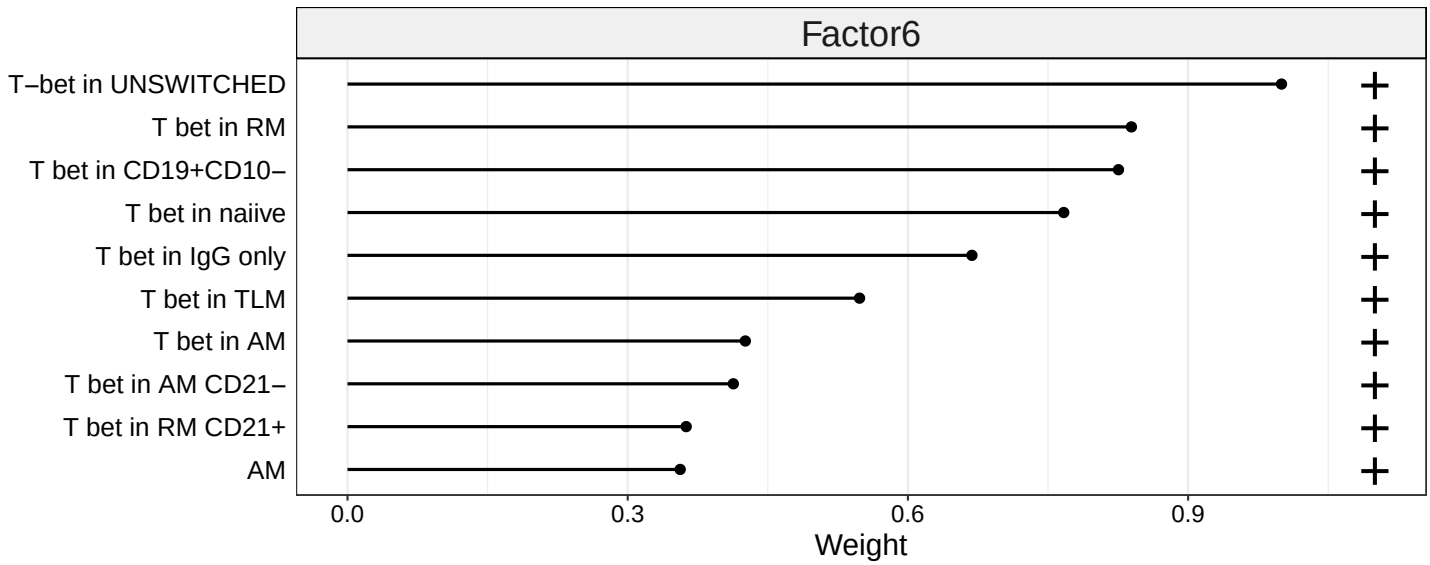

Supplementary Fig. 6 MOFA analysis. a) Factors values distribution in PRNT- and PRNT+. b) B cells population contributing to the variance of factor 6.

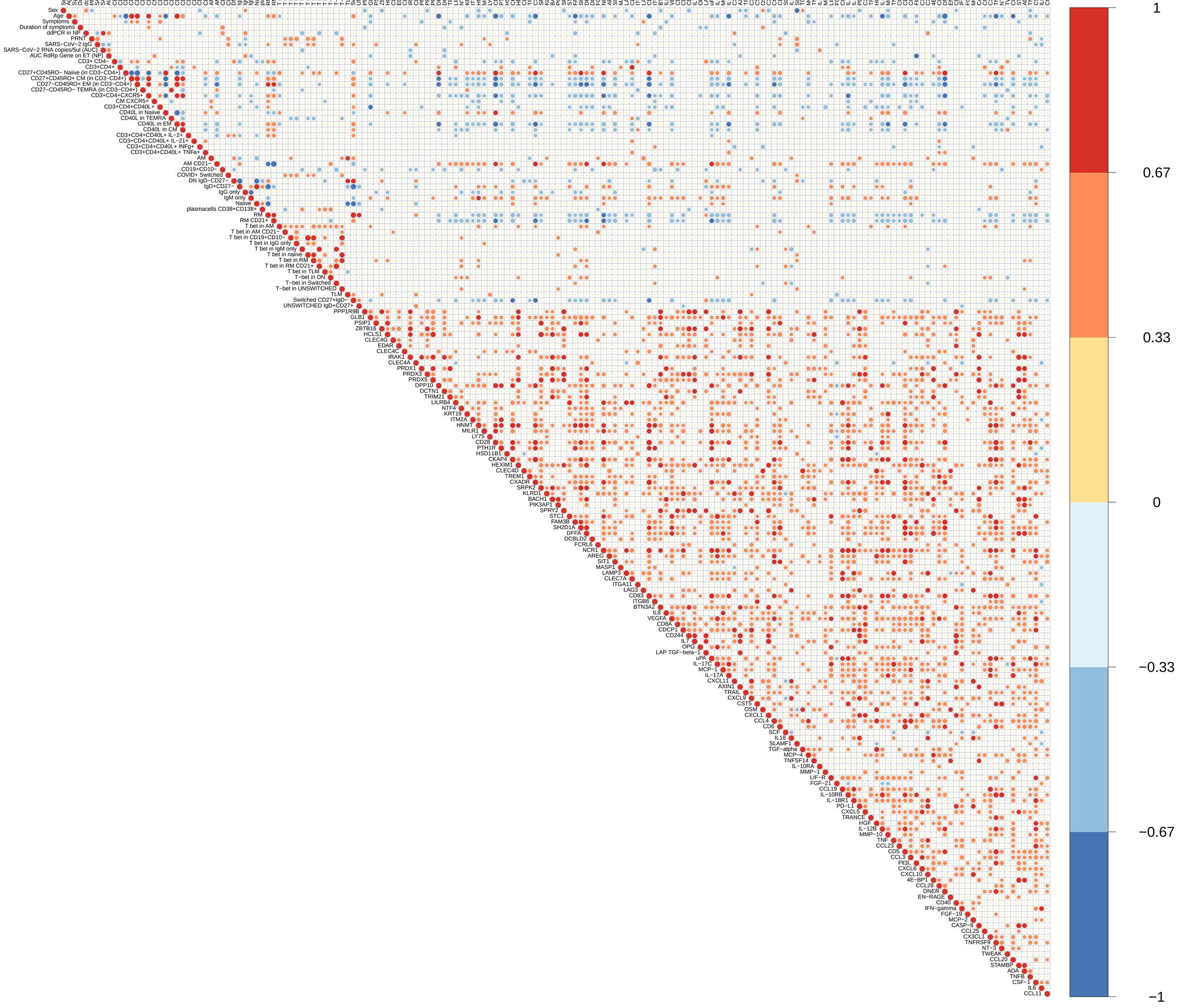
Sex
Age
Symptoms
Duration of symptoms
ddPCR in NP
PRNT
SARS−CoV−2 IgG
SARS−CoV−2 RNA copies/5ul (AUC)
AUC RdRp Gene on ET (NP)
CD3+ CD4−
CD3+CD4+
CD27+CD45RO− Naiive (in CD3−CD4+)
CD27+CD45RO+ CM (in CD3−CD4+)
CD27−CD45RO+ EM (in CD3−CD4+)
CD27−CD45RO− TEMRA (in CD3−CD4+)
CD3+CD4+CXCR5+
CM CXCR5+
CD3+CD4+CD40L+
CD40L in Naiive
CD40L in TEMRA
CD40L in EM
CD40L in CM
CD3+CD4+CD40L+ IL−2+
CD3+CD4+CD40L+ IL−21+
CD3+CD4+CD40L+ INFg+
CD3+CD4+CD40L+ TNFa+
AM
AM CD21−
CD19+CD10−
COVID+ Switched
DN IgD−CD27−
IgD+CD27−
IgG only
IgM only
Naiive
plasmacells CD38+CD138+
RM
RM CD21+
T bet in AM
T bet in AM CD21−
T bet in CD19+CD10−
T bet in IgG only
T bet in IgM only
T bet in naiive
T bet in RM
T bet in RM CD21+
T bet in TLM
T−bet in DN
T−bet in Switched
T−bet in UNSWITCHED
TLM
Switched CD27+IgD−
UNSWITCHED IgD+CD27+
PPP1R9B
GLB1
PSIP1
ZBTB16
HCLS1
CLEC4G
EDAR
CLEC4C
IRAK1
CLEC4A
PRDX1
PRDX3
PRDX5
DPP10
DCTN1
TRIM21
LILRB4
NTF4
KRT19
ITM2A
HNMT
MILR1
LY75
CD28
PTH1R
HSD11B1
CKAP4
HEXIM1
CLEC4D
TREM1
CXADR
SRPK2
KLRD1
BACH1
PIK3AP1
SPRY2
STC1
FAM3B
SH2D1A
DFFA
DCBLD2
FCRL6
NCR1
AREG
SIT1
MASP1
LAMP3
CLEC7A
ITGA11
LAG3
CD83
ITGB6
BTN3A2
IL8
VEGFA
CD8A
CDCP1
CD244
IL7
OPG
LAP TGF−beta−1
uPA
IL−17C
MCP−1
IL−17A
CXCL11
AXIN1
TRAIL
CXCL9
CST5
OSM
CXCL1
CCL4
CD6
SCF
IL18
SLAMF1
TGF−alpha
MCP−4
TNFSF14
IL−10RA
MMP−1
LIF−R
FGF−21
CCL19
IL−10RB
IL−18R1
PD−L1
CXCL5
TRANCE
HGF
IL−12B
MMP−10
TNF
CCL23
CD5
CCL3
Flt3L
CXCL6
CXCL10
4E−BP1
CCL28
DNER
EN−RAGE
CD40
IFN−gamma
FGF−19
MCP−2
CASP−8
CCL25
CX3CL1
TNFRSF9
NT−3
TWEAK
CCL20
STAMBP
ADA
TNFB
CSF−1
IL6
CCL11
1
0.67
0.33
0
−0.33
−0.67
−1

Table 2. Table of different Symptoms at admission of the PRNT +, PRN- and SARS-CoV-2 negative patients.

Symptoms	**PRNT+** (n=25)	**PRNT-** (n=11)[a]	**SARS-CoV-2 neg** (n=11)
Respiratory**, n/tot (%)**	10/25 (40%)	4/11 (36%)	7/11
Gastrointestinal**, n/tot (%)**	5/25 (20%)	3/11 (27%)	4/11 (36%)
Convulsion**, n/tot (%)**	2/25 (8%)	1/11 (9%)	1/11 (9%)
Migraine**, n/tot (%)**	5/25 (20%)	3/11(27%)	1/11 (9%)
Fever > 37.5**, n/tot (%)**	10/25 (40%)	6/11 (54%)	11/11 (100%)
Fever < 37.5**, n/tot (%)**	4/25 (16%)	3/11(27%)	0/11 (0%)
Skin rash**, n/tot (%)**	0/25 (0%)	1/11 (9%)	2/11 (18%)
Conjunctivitis**, n/tot (%)**	3/25 (12%)	1/11 (9%)	2/11 (18%)
Joint pain**, n/tot (%)**	3/25 (12%)	2/11 (18%)	1/11 (9%)
Prescriptions/Treatments			
Azithromycin, n/tot (%)	6/25 (24%)	2/11	0/8[b] (0%)
Plaquenil, n/tot (%)	6/25 (24%)	4/11 (36%)	n.a.
Corticosteroids, n/tot (%)	2/24[b] (17%)	1/11 (9%)	1/8[b] (13%)
Anakirna, n/tot (%)	1/25 (4%)	0/11 (0%)	n.a.

[a]For 6 samples detailed symptoms history was not available; [b]information not available for all the individuals of the group. na=not available.